SHOCK TUBE INVESTIGATION OF PRESSURE AND ION SENSORS USED IN PULSE DETONATION ENGINE RESEARCH

THESIS

Robert J. McMillan, Ensign, USNR

AFIT/GAE/ENY/04-J07

DEPARTMENT OF THE AIR FORCE
AIR UNIVERSITY

AIR FORCE INSTITUTE OF TECHNOLOGY

Wright-Patterson Air Force Base, Ohio

The views expressed in this thesis are those of the author and do not reflect the official policy or position of the United States Navy, United States Air Force, Department of Defense, or the United States Government.

AFIT/GAE/ENY/04-J07

SHOCK TUBE INVESTIGATION OF PRESSURE AND ION SENSORS USED IN PULSE DETONATION ENGINE RESEARCH

THESIS

Presented to the Faculty

Department of Aeronautics and Astronautics

Graduate School of Engineering and Management

Air Force Institute of Technology

Air University

Air Education and Training Command

In Partial Fulfillment of the Requirements for the

Degree of Master of Science in Aeronautical Engineering

Robert J. McMillan, BS

Ensign, USNR

June 2004

AFIT/GAE/ENY/04-J07

SHOCK TUBE INVESTIGATION OF PRESSURE AND ION SENSORS USED IN PULSE DETONATION ENGINE RESEARCH

Robert J. McMillan, BS
Ensign, USNR

Approved:

Dr. Paul I. King (Chairman)	date
Dr. Ralph A. Anthenien (Member)	date
Dr. Mark F. Reeder (Member)	date

Abstract

Shock tubes utilize a difference in pressures between gases separated by a diaphragm to create a shock wave when the diaphragm ruptures. By using sensors of known spacing, the speed of the wave can be determined. The AFIT 2-inch shock tube was reassembled and tested to ensure proper and safe operation. A high-speed data acquisition system was configured to take data at 2 MS/s. This research showed that the Mach number of the shock waves produced in this shock tube fall within 7% of theoretical values at speeds under Mach 3 and within 9% at higher speeds. The peak velocity of each shock wave was shown to occur at approximately 3 meters from the diaphragm.

The second portion of the research focused on the testing of sensors used to evaluate the performance of the pulse detonation engine (PDE) for research and developmental purposes. The high temperatures of the PDE are too harsh for unaltered dynamic pressure transducers to provide accurate pressure measurements. Therefore, two alternatives were developed: coat the sensors with a 0.6 mm thick insulating silicone that protects them from the heat and detect the waves by detecting ions in the combustion inside the PDE tubes with spark plugs instead of measuring pressure. However, neither the effect of putting this coating on the sensors nor the sensitivity of the spark plug as an ion sensor were known. This researched proved that no degradation in response time, rise time, or sensitivity results from coating the pressure transducers with silicone. The research also found that the ion sensors are unable to consistently detect ions created by a Mach 8 shock wave through air suggesting that ions detected in the PDE most likely result from combustion only.

Acknowledgments

I would like to begin by extending a sincere thanks to my advisor, Dr. Paul King, and my technical advisor, Capt. Colin Tucker, USAF, for their help and guidance throughout the project. I would like to thank my readers, Dr. Ralph Anthenien and Dr. Mark Reeder, for their helpful and insightful suggestions of improvements and modifications to my work.

I would like to thank Jeff Stutrud for developing the data acquisition software and all those in the Pulse Detonation Research Facility for providing technical advise as well as hardware necessary for successful completion. I would also like to thank those in the AFIT labs for their consultation and help in the design of the experiment. I would most especially like to thank Dwight Gehring for his extensive work and devotion to setting up the shock tube for experimental research and ensuring that all systems were operating properly. Without his work, this project would not have been possible.

Finally, I would like to thank my wife. Her tolerance of my long hours showed her gracious and loving nature, and the distraction she provided was an invaluable tool that helped me to refocus my efforts.

Robert J. McMillan

Matthew 19:26

Table of Contents

List of Figures

List of Tables

Nomenclature

Abbreviations

AFIT	Air Force Institute of Technology
AFRL	Air Force Research Laboratory
Ar	argon
DAQ	data acquisition system
H_2	diatomic hydrogen
He	helium
O_2	diatomic oxygen
O	monatomic (dissociated) oxygen
N_2	diatomic nitrogen
N	monatomic (dissociated) nitrogen
NO	nitric oxide
PDE	pulse detonation engine
RC	resistor – capacitor electrical circuit
RTV	room temperature vulcanizing

Standard Symbols

a	speed of sound
M	Mach number
MW	molecular weight
P	pressure
R	specific gas constant
T	temperature
V	velocity

Greek Symbols

γ	specific-heat ratio [unitless]
ρ	density [kg/cm^3]

Subscripts

s	incident shock
R	reflected shock
1	low pressure region in front of shock wave
2	region between shock wave and contact surface
3	region between expansion wave and contact surface
4	high pressure region in front of expansion wave
5	region behind reflected shock wave
6	region behind reflected expansion wave

SHOCK TUBE INVESTIGATION OF PRESSURE AND ION SENSORS USED IN PULSE DETONATION ENGINE RESEARCH

1 Introduction

1.1 General

In an age where much of fluid dynamics research has turned to computational analysis, there remains some research that cannot be completed with a computer. This is the case in this set of experiments where the response of different sensors detecting changes in pressure and the ionization of gases must be characterized in a way that allows the researchers using the sensors to make more bold conclusions about the data the sensors provide. In this experiment, a shock tube is used to analyze the performance of these sensors.

1.2 Purpose

In recent years, the military has begun searching for an alternative to gas turbine engines for one-time use applications such as missiles. The engine which has risen to the forefront due to its low cost, low weight, high thrust potential, and scalability is the Pulse Detonation Engine (PDE). While the PDE is mechanically simple, the technology behind it requires a significant amount of research and development (Panzenhagen, 2004:1)

The PDE consists of a series of combustion tubes which are closed at one end, filled with a gaseous fuel-air mixture, and ignited to produce a combustion wave. When combustion occurs in these tubes, a pulse of thrust is produced, and when that

combustion transitions into a detonation, the thrust is much greater. By forcing the tubes to detonate in series at a rate upwards of 100 detonations per second, constant thrust is effectively produced (Panzenhagen, 2004:2).

Recent research has focused on the sequence of events inside the tube, specifically during the ignition and detonation. The performance of the PDE and the existence of a detonation inside its thrust tubes are determined by measuring the wave speed in the tube. Due to the extreme temperatures, simple dynamic pressure transducers to detect the sharp rise in pressure of a shock wave cannot continue operating for more than a few seconds (Zdenek and Anthenien, 2004:1). To solve this problem, room temperature vulcanizing (RTV) silicone was used to coat the ends of the transducers to insulate them from the heat. In addition, ion sensors were developed from spark plugs to detect the ionization of gases in the combustion event which propagates behind the shock wave. However, the assertions which can be made about the performance of the engine are limited when using these two instruments because experiments have not been conducted to determine their effectiveness compared to standard pressure transducers. In the case of the ion probe, research must be conducted to ensure that the ions are not being created by the shock wave which traverses the tube prior to the detonation wave.

The purpose of this project is twofold. The first is to establish a relationship between the output of an unaltered dynamic pressure transducer and that of a pressure transducer coated with a thin (0.6 mm) layer of RTV. The second is to determine if the ion sensor probes are sensitive enough to detect the ions created by a shock wave – representative of those seen in the PDE – through air. While similar experiments were conducted by Laderman, Hecht, Stern, and Oppenheim, their experiments utilized an ion

sensor where the sensing electrodes consisted of concentric metal rings rather than the automotive sparkplug used in this research. In addition, the experiments used various mixtures of hydrogen, oxygen, and nitrogen rather than using atmospheric air (Laderman et al., 1960:203). The results of this research will allow the researchers working with the pulse detonation engine to make stronger assertions about the characterization of the detonation wave and hence the performance of the engine.

This research is in direct support of the Air Force Research Laboratory Propulsion Directorate, Turbine Engine Division, Combustion Sciences Branch, Wright-Patterson AFB, Ohio and the Air Force Office of Scientific Research. The research was conducted in the Wind Tunnel / Shock Tube Laboratory in Building 644 of the Air Force Institute of Technology, Wright-Patterson AFB, OH.

1.3 Background

Shock tubes operate by using differential pressure to create a shock wave. This is completed by separating two sections of the shock tube – one with high pressure and one with low pressure – with a thin piece of metal or plastic called a diaphragm (Glass, 1958:1). As the pressure builds, more stress is placed on the diaphragm until it bursts. After the burst, a shock wave flows down the low pressure end of the tube called the expansion chamber or driven section while a rarefaction wave flows down the high pressure end of the tube known as the compression chamber or driver section. These waves equalize the pressure in the tube (Wright, 1961:30).

Although the first shock tube was used by Paul Vieille in France in 1899 (Glass, 1958:1), shock tubes did not come into general use until the blast wave studies of World

War II (Wright, 1961:1). Because of the controlled environment and relatively low cost of experiments, shock tubes have become a valuable tool in investigating many different aspects of high speed fluid and gas dynamics. Shock tubes have been used to develop the laws of reflection for shock and expansion waves, investigate shock diffraction, study gas dynamics at high temperatures, study detonations, and act as high speed wind tunnels for supersonic and hypersonic flow research (Glass, 1958:2),(Wright, 1961:2).

While the AFIT 2-inch shock tube has been in sporadic use since at least 1969 (Vlcek, 1994:2), it has been in storage for nearly ten years. In order to conduct the research for this project, the shock tube was brought out of storage, reassembled, and tested to determine the proper methods for operating the tube. Because no prior record of operating procedures exists, new procedures were developed to ensure safe and efficient use. Modern instrumentation and a new, high-speed data acquisition system were also installed and configured for use on the tube. Through these efforts, it should now be possible for future research on the shock tube to be conducted more effectively.

1.4 Problem Statement

This research addresses two sensor uncertainties involved in experimentation on the PDE. First, the data obtained from the pressure transducers coated with RTV silicone must be as accurate and precise as the data obtained with pressure transducers absent of any coating. Second, the output from the ion sensor probes must be the result of the combustion inside the tubes of the PDE and not the result of the shock wave which precedes the combustion wave.

The harsh environment created by the high temperatures and vibrations of the PDE prevents the use of conventional piezoelectric dynamic pressure transducers. The recessed portion of the transducer can be filled with a 0.6 mm thick RTV silicone coating to protect the sensor for a short period of time but the effect of this coating on the response of the transducer is unclear (Zdenek and Anthenien, 2004:1). Assumptions have been made that this coating causes a degradation in the sensitivity of the sensors but no research has been conducted to determine and quantify the true effect.

The PDE generates thrust by directing the pressure rise from a combustion event down a tube and exhausting it to atmosphere creating a pulse of thrust. This combustion event is produced by igniting a vaporized fuel inside the tube. As the combustion event accelerates down the tube, it transitions from a deflagration to a detonation (Panzenhagen, 2004:2-1). This detonation sends a shock wave ahead of it which induces flow and preheats the vapors. In order to determine the effect of the shock wave which precedes the combustion on the sensors, the concentration of ions necessary for detection by the ion probe in a shock wave must be established (Laderman et al., 1960:199).

Whether a deflagration or a detonation, the combustion event is a chemical reaction which produces ions from the reactants in order to form the final products. When the ions interact with the ion sensor, the circuit is connected and the electrode discharges (Tucker et al., 2003). The rate of discharge can be used to determine the pressures in the tube (Zdenek, 2004:85). This makes the sensor an invaluable tool in measuring the events in the PDE tubes provided that it is clear what event is creating the detectable ions. The complexity of ion generation makes it difficult to predict the creation of ions (Zdenek and Anthenien, 2004:4). For this reason, tests must be

conducted to determine if the shock wave itself causes temperatures high enough to generate ions in air.

1.5 Objectives

The objective of this research is to use the AFIT 2-inch shock tube to characterize the performance of sensors in use on the PDE. The following tasks were completed:

1. Re-commission the AFIT 2-inch shock tube for experimental research and develop operating and safety procedures for its use.
2. Examine the response of four piezoelectric dynamic pressure transducers to determine the characteristic response of each sensor without a coating and install the sensors at different locations to determine wave speed.
3. Examine the response of two sensors coated with RTV silicone compared to two without a coating.
4. Examine the response of ion sensor probes to hypersonic shock waves in air.

1.6 Chapter Summary

A shock tube provides an inexpensive method of testing instruments in a controlled environment to determine specific response characteristics. The environment of a PDE is not well suited for measurement by standard piezoelectric pressure transducers. Different or modified instruments with known characteristics must be used to measure the combustion events inside the PDE. This research examines the response of two alternative sensors for use in the PDE. First, the response of a piezoelectric dynamic pressure transducer coated with RTV silicone to a shock wave will be compared

to the response of the same type of transducer without a coating. Second, ion sensor probes will be tested to determine if they are capable of detecting the ionization of air behind a hypersonic shock wave.

2 Theory

2.1 Introduction

A shock tube functions by forcing two different pressures to equalize at high speeds creating both a shock wave and a rarefaction or expansion wave. This chapter outlines the theory behind the operation of a shock tube including characteristic equations which describe the events within the tube. In addition, discussions of detonations, shock tube gas chemistry, and the use of gases other than air are followed by a description of CHEMKIN, a program used to simulate events in a shock tube with real gas effects.

2.2 Shock Tube Theory

The shock tube is formed by two closed sections of a single tube separated by a diaphragm in the center. When the pressure difference between the two sections becomes sufficient, the diaphragm ruptures and a normal shock wave is sent down the low pressure driven section while an expansion fan or rarefaction wave is sent down the high pressure driver section. The gases in the two sections need not be the same and can be set to different temperatures. The shock wave causes a mass motion and forces the pressure in the driven section to rise along with the temperature, and the expansion wave decreases the pressure and temperature in the driver section (Anderson, 2003:265). Figure 2-1 displays the regions of the shock tube prior to the diaphragm's rupture.

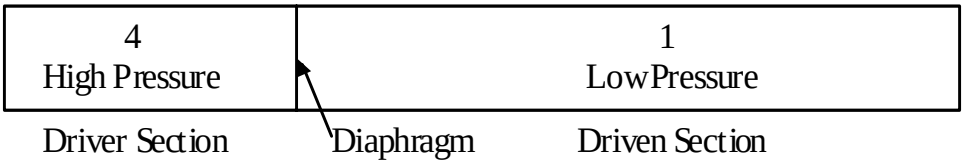

Figure 2-1: Shock Tube Regions Before Diaphragm Burst

The point at which the driver and driven gases meet and begin mixing is referred to as the contact surface. This contact surface along with the remainder of the region between the expansion fan and the normal shock moves at the same velocity and is the mass motion induced by the normal shock (Wright, 1961:30). The contact surface divides regions 2 and 3. Across it, pressure and velocity are constant while temperature, density, and entropy change (Anderson, 2003:265). Figure 2-2 shows the regions in the shock tube immediately following the rupture of the diaphragm.

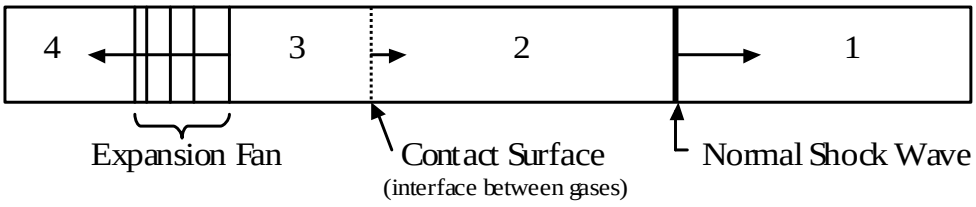

Figure 2-2: Shock Tube Regions After Diaphragm Burst

When the normal shock wave reaches the closed end of the tube, it reflects and propagates back toward the opposite end of the tube (Wright, 1961:30). The reflected normal shock wave stops the mass motion of the gas regardless of the strength of the incident shock wave. This is to say that the speed of the reflected shock wave can be determined by setting the gas velocity to zero (Anderson, 2003:273). Because the incident normal shock pressurized and preheated the gas in the driven section, this

reflected wave is responsible for a larger increase in pressure and temperature than the incident shock. Often, it is this reflected wave which causes the air to dissociate and possibly ionize.

Likewise, the expansion fan reflects and moves back toward the center. When the reflected expansion fan reaches the reflected shock, both waves will reflect off of each other and propagate toward opposite ends of the tube. This process continues until the tube reaches a steady state pressure and temperature which typically takes less than one second (Wright, 1961:30).

2.3 Shock Tube Analytical Solution – Ideal Gas Assumptions

The general equations for the performance of a shock tube are easily derived using the following series of assumptions: the gases are perfect gases with constant specific heats, the flow is one dimensional, there is no viscosity or heat transfer, and the diaphragm burst is perfect. A perfect or ideal gas is a gas which follows the equation $P = \rho RT$ and is generally applied to gases at low temperatures and pressures (Cengel and Boles, 2002:88). A non-ideal or real gas does not follow this equation at sufficiently high temperature or pressure (Cengel and Boles, 2002:622). This is the case when the shock mach numbers approach hypersonic speeds. Section 2.4 outlines the effects real gases have on the ideal gas equations in this section. While not as accurate as the real-gas shock tube solution, the equations developed from these assumptions are simple and easy to apply and very closely describe shock tube behavior up to Mach 3. Beyond that point, the equations may still be used as a general guide (Hall, 1958:142).

There are two primary parameters that determine the strength of the shock: the pressure ratio between the driver section and the driven section (P_4/P_1), and the speed of sound ratio between the driver section and the driven section (a_4/a_1) (Hall, 1958:142). The speed of sound ratio is determined by the ratios of specific heats and the molecular weights of the gases used in the driver and the driven sections. Figure 2-3 depicts the conditions in the shock tube prior to the rupture of the diaphragm assuming that neither side of the shock tube is heated or cooled.

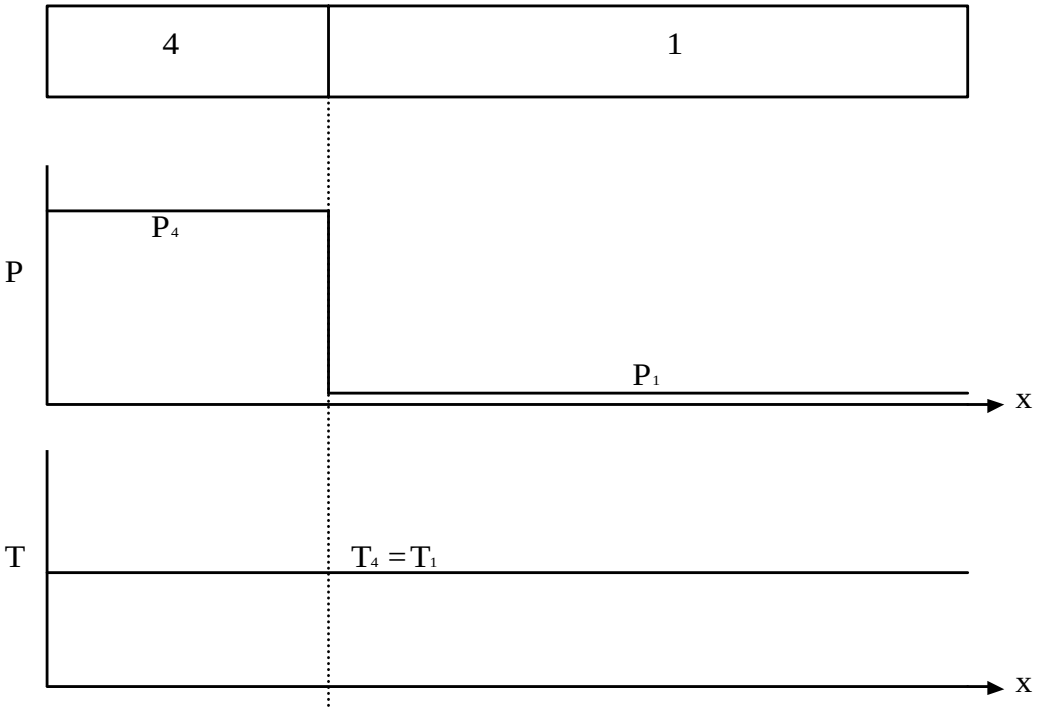

Figure 2-3: Conditions in Shock Tube Before Diaphragm Burst

The equations can be derived beginning with the equations for continuity, momentum, and energy as found in Anderson's *Modern Compressible Flow* (Anderson, 2003:266-298). The principles of a moving normal shock are used to develop the relationship between regions 1 and 2 on either side of the shock wave and between

regions 3 and 4 on either side of the expansion wave. Figure 2-4 shows the conditions in the shock tube following the rupture of the diaphragm. The contact surface properties discussed in section 2.2 are used to unite the two portions of the relations and complete equations for the entire system. The equations to follow are obtained from Anderson's derivation (except where otherwise noted).

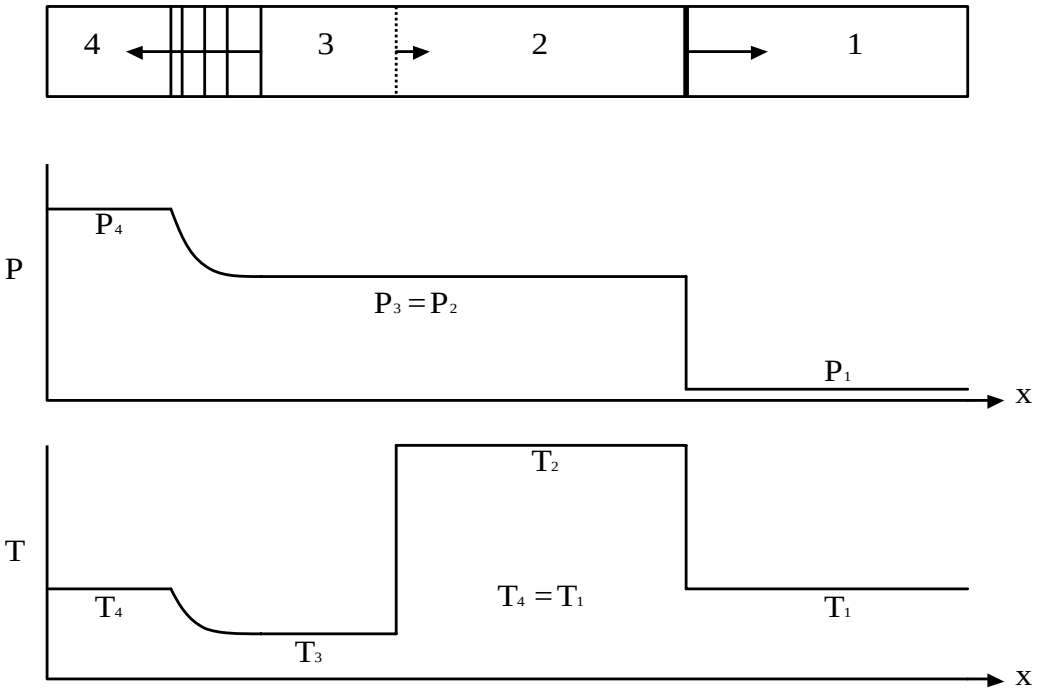

Figure 2-4: Conditions In Shock Tube After Diaphragm Burst

Although there are only two gases in the tube initially, after the bursting of the diaphragm, there are essentially four gas states as the properties of each region are different including temperature, density, and pressure as well as the ratio of specific heats when the shock is of sufficient strength. The speed of sound for each gas state should be calculated using the equation

$$a = \sqrt{\gamma RT} \qquad [1]$$

where ratio of specific heats and the gas constant are unique to the gas, and the temperature is the gas temperature inside that portion of the tube before the diaphragm bursts. With the pressure in each section of the tube recorded before the diaphragm bursts, the Mach number can be calculated using the following relationship given by (Hoffmann and Chiang, 2000:154)

$$\frac{P_4}{P_1} = \frac{\gamma_1 - 1}{\gamma_1 + 1}\left[\frac{2\gamma_1}{\gamma_1 - 1} M_s^2 - 1\right]\left[1 - \frac{\frac{\gamma_4 - 1}{\gamma_4 + 1}\left(\frac{a_1}{a_4}\right)\left(M_s^2 - 1\right)}{M_s}\right]^{-\frac{2\gamma_4}{\gamma_4 - 1}} \quad [2]$$

where M_s is the Mach number of the shock wave, subscript 1 denotes properties in the driven section, and subscript 4 denotes properties in the driver section.

With the Mach number known, the ratio of pressures on either side of the shock (P_2/P_1) can be calculated using the normal shock relation

$$\frac{P_2}{P_1} = 1 + \frac{2\gamma_1}{\gamma_1 + 1}\left(M_s^2 - 1\right). \quad [3]$$

This pressure ratio can then be used to determine the temperature ratio on either side of the shock wave using

$$\frac{T_2}{T_1} = \frac{P_2}{P_1}\left(\frac{\frac{\gamma_1 + 1}{\gamma_1 - 1} + \frac{P_2}{P_1}}{1 + \frac{\gamma_1 + 1}{\gamma_1 - 1}\frac{P_2}{P_1}}\right) \quad [4]$$

The temperature on the back side of the shock wave can be used to predict the dissociation and ionization of air. This will be discussed later in section 2.6.

The relationship of pressure ratio to Mach number of the shock is asymptotic. Therefore, for any fixed pair of gases, there is a theoretical maximum Mach number that

can be reached. This theoretical maximum Mach number, indicated by a star superscript, is given by (Hall, 1958:142)

$$M_s^* = \frac{\gamma_1 + 1}{2(\gamma_4 - 1)} \frac{a_4}{a_1} + \sqrt{\left[\frac{\gamma_1 + 1}{2(\gamma_4 - 1)} \frac{a_4}{a_1} \right]^2 + 1} \qquad [5]$$

This equates to Mach 6.16 for air to air and Mach 10.6 for a helium driver into a driven section of air.

The speed of the reflected shock wave is entirely dependent on the speed of the incident shock wave by the relation

$$\frac{M_R}{M_R^2 - 1} = \frac{M_s}{M_s^2 - 1} \sqrt{1 + \frac{2(\gamma_1 - 1)}{(\gamma_1 + 1)^2} (M_s^2 - 1) \left(\gamma_1 + \frac{1}{M_s^2} \right)} \qquad [6]$$

The following equations are written as derived by (Gaydon and Hurle, 1961:24-26). As has been previously stated, the reflected shock travels at a higher velocity and raises the pressure and temperature higher than the incident shock. Figure 2-5 displays the conditions in the shock tube as the reflected shock approaches the center.

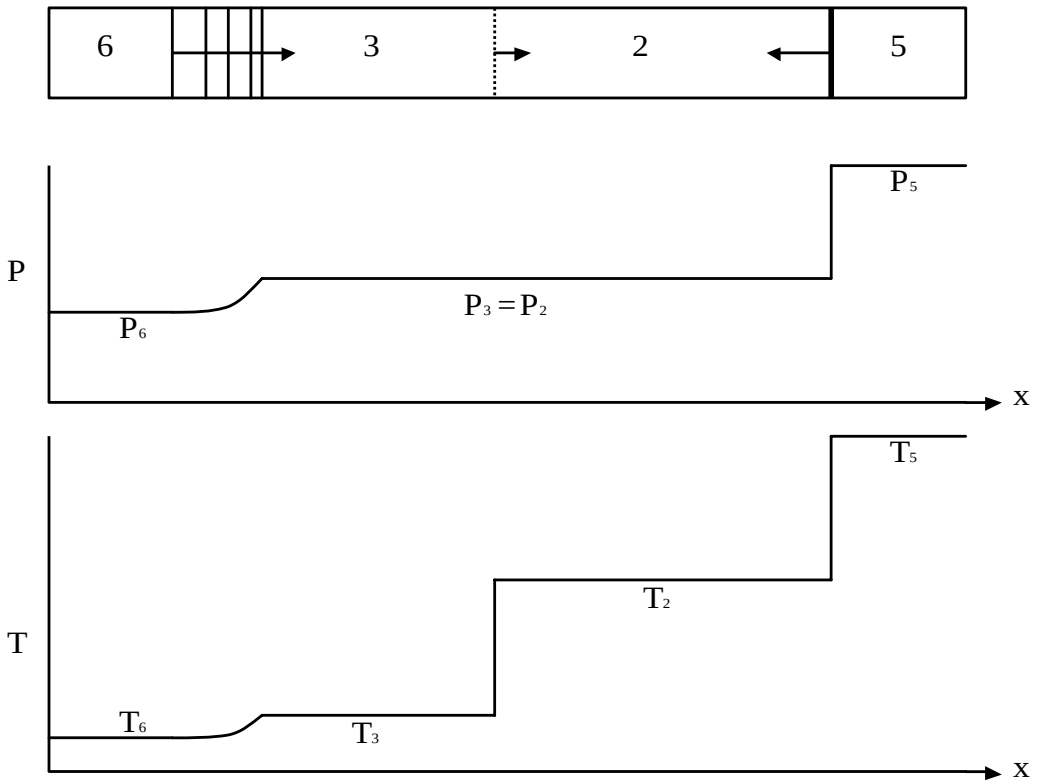

Figure 2-5: Conditions in Shock Tube After Shock and Expansion Reflections

Recall from equation 3 that the pressure rise behind the shock wave is dependent on the speed of that shock. The same is true for the reflected shock. Therefore, equation 3 can be modified to show that

$$\frac{P_5}{P_2} = 1 + \frac{2\gamma_1}{\gamma_1 + 1}\left(M_R^2 - 1\right) \qquad [7]$$

The reflected shock wave stops all mass motion (gas particle motion) so that the velocity behind the reflected shock is zero. The velocity in front of the incident shock was also zero leaving the mass motion relations as

$$V_2 = \frac{2a_1}{\gamma_1 + 1}\left(M_s - \frac{1}{M_s}\right) = \frac{2a_2}{\gamma_1 + 1}\left(M_R - \frac{1}{M_R}\right) \qquad [8]$$

Notice that in these equations, the ratio of specific heats did not change but the speed of sound did. This is a result of the static temperature rise across the first shock. The gas through which the reflected shock is propagating is still the same gas that was originally in the driven section. This is true until the reflected shock reaches the contact surface where the two gases are mixing. Cases where this assumption may fail are when the initial shock wave is of sufficient strength to cause the air to dissociate or to cause a chemical reaction between the gases (e.g. combustion between hydrogen and oxygen at high mach numbers) in which case all the ideal gas equations will fail.

While the Mach number of the reflected shock wave has been calculated, the actual speed of the wave has yet to be determined. The speed relative to the motion of the particles in the tube is a simple calculation using the Mach relation $M=V/a$. However, the calculation of the true speed of the wave must take into account the mass motion of the gases behind the incident shock wave. Therefore, the equation for the velocity of the wave becomes

$$V_R = M_R a_2 - V_2 \qquad [9]$$

To determine the pressure ratio across the reflected shock with only information from the incident shock, equations 7 and 8 can be solved for P5/P2 to yield

$$\frac{P_5}{P_2} = \left(\frac{\frac{\gamma_1 + 1}{\gamma_1 - 1} + 2 - \frac{P_1}{P_2}}{1 + \frac{\gamma_1 + 1}{\gamma_1 - 1}\frac{P_1}{P_2}} \right) \qquad [10]$$

With the pressure ratio known, the temperature ratio may now be solved by

$$\frac{T_5}{T_2} = \frac{P_5}{P_2}\left(\frac{\frac{\gamma_1+1}{\gamma_1-1}+\frac{P_5}{P_2}}{1+\frac{\gamma_1+1}{\gamma_1-1}\frac{P_5}{P_2}}\right) \qquad [11]$$

The temperature and pressure behind the reflected shock may now be calculated knowing only the Mach number of the incident shock wave. This value can be determined from the speed of sound of the driven gas and the velocity of the wave as determined from the instruments with known spacing in the experiment.

2.4 Real Shock Tube Behavior – Real Gases

While the equations do a reasonable job of predicting the conditions in the shock tube, a large number of assumptions were made in order to derive them. In reality, the departure from the ideal conditions occurs immediately. After the diaphragm bursts, it does not disappear. Instead, portions of it remain around the diameter of the tube obstructing the flow and slowing the mass motion. When the diaphragm bends before bursting, it breaks in a way that sends some of the air directly at the walls of the tube – a far cry from the model of one dimensional flow. To counter this, Wright recommends using an expansion chamber between the diaphragm and the test section with a length that is at least 20 times the diameter of the tube (Wright, 1961:36). For a two inch tube that would mean a length of at least 1.01 m (40 in.). The test section in this experiment begins 1.63 m (64 in.) downstream of the diaphragm satisfying this requirement.

Another assumption made was that the gases behave as perfect gases and have constant specific heats. This is true when the gases are at room temperature prior to the

bursting of the diaphragm. However, as the shock wave heats the air in the tube, it behaves less like a perfect gas. While the pressure trends remain largely the same as the ideal relations related to Mach number, the temperature ratio increases at a much slower rate and density increases much faster (Gaydon and Hurle, 1961:31). When the temperature becomes high enough to dissociate the gas, the trends depart even further from the ideal model. This concept is discussed further in section 2.6. In addition, the rapid pressure and temperature changes will not leave the specific heats constant. High temperatures cause molecular vibrations that causes the ratio of specific heats to decrease (Gaydon and Hurle, 1961:30).

The assumption was made that there was no viscosity or heat transfer. In viscous flow, all the gas does not mix at the contact surface because there can be no flow at the wall. Instead, a thin boundary layer of the unmixed gases is left to mix well after the contact surface passes (Gaydon and Hurle, 1961:71). Because this research focuses on the effects on the gas prior to the arrival of the contact surface and gas mixing at the sensors, the inviscid assumption should not detract from the data. The heat transfer assumption is not as accurate. The gases inside the tube are heated to, in some cases, several thousand degrees. It is not possible for the gases to reach these temperature without transmitting at least some of the heat to the one inch thick stainless-steel wall surrounding the gases.

In general, the equations accurately predict shock tube performance up to Mach 3. They do not predict the attenuation seen in strong shock waves (Hall, 1958:159).

2.5 Use of Gases other than Air

Recall from section 2.3 that the performance of the shock tube is based entirely upon the ratios P_4/P_1 and a_4/a_1. Therefore, parameters that may change the performance of the tube are changing the pressure, temperature, or the gas in either side of the tube. From the equation 5, there is a maximum Mach number for any given pair of gases. To achieve higher Mach numbers, the gases must be changed. Because the strength of the shock increases as the ratio of speeds of sound increases, it is desirable to have a driver gas with a low molecular weight and – because it appears in other parts of the analytical equations – a low ratio of specific heats (Hall, 1958:143). Conversely, it is desirable to have a driven gas with a high molecular weight (Anderson, 2003:298). Put simply, the strongest shock wave is obtained by using a heavy driven gas and a light driver gas.

To meet these recommendations, many experiments use either hydrogen or helium as the driver gas. While hydrogen is lighter and capable of producing higher Mach numbers, it also attenuates at almost twice the rate of helium and is considerably more hazardous. The rate of decay of the shock strength increases as the speed of sound of the driver increases. However, the pressures before the diaphragm bursts has no known effect on this rate of attenuation (Hall, 1958:160). This attenuation is a result of the boundary layer viscous effects which sap the kinetic energy and momentum from the driver gas (Gaydon and Hurle, 1963:73). Because this research seeks to achieve a high temperature from the reflected wave, the helium was chosen for its lower attenuation. In addition, at high Mach numbers when hydrogen is used as a driver with air as the driven gas, combustion may occur between the hydrogen and the oxygen (Hall, 1958:143). It was not the focus of this work to generate a detonation wave.

To meet the recommendations for the driven section, many past experiments have used argon due to its higher molecular mass compared to air. As previously stated, as the molecular weight of the gas in the driver section decreases, the attenuation of the shock wave through the driven gas increases. This is due to the increase in the ratio of the molecular weights with a light gas penetrating a heavy gas. Due to the same principle, as the molecular weight of the gas in the driven section increases, the attenuation of the shock increases (Gaydon and Hurle, 1963:73). It is therefore impractical to use gases much heavier than argon and the gain in shock Mach number from the use of argon is not sufficient to warrant switching gases from readily available air (Glass and Hall, 1959:413). Table 2-1 shows maximum possible Mach numbers using various combinations of test gases given that the pressure ratio goes to infinity.

Maximum Theoretical Mach Numbers for Various Gas Combinations							
Driver Gas (4)	Driven Gas (1)	MW_4	MW_1	γ_4	γ_1	A_4/A_1	M_s*
Air	Air	28.95	28.95	1.404	1.404	1	6.16
He	Air	4.003	28.95	1.667	1.404	2.93	10.6
He	N_2	4.003	28.02	1.667	1.404	2.88	10.4
He	Ar	4.003	39.94	1.667	1.667	3.16	12.7
H_2	Air	2.016	28.95	1.407	1.404	3.8	22.5
H_2	N_2	2.016	28.02	1.407	1.404	3.73	22.1
H_2	Ar	2.016	39.94	1.407	1.667	4.09	26.8

Table 2-1: Max Theoretical Mach Number for Test Gas Combinations when $P_{41} \rightarrow \infty$

2.6 High Temperature Gas Dynamics

As the incident and reflected shocks propagate down the shock tube, the air in the tube is heated by each pass causing it to depart from ideal gas behavior. In fact, as the gas approaches 2500 K, the oxygen molecules in the air begin to dissociate (Anderson, 1989:374).

The diatomic oxygen and nitrogen molecules that comprise the majority of the air can be described as a dumbbell: two atoms linked together by a single bond. When the molecules reach sufficient temperature, this dumbbell begins to rotate. As the temperature continues to rise, the rotation speed increases until the rotational energy is fully excited. This term fully excited does not mean that no additional energy can be absorbed because as the temperature increases further, the molecule then begins to vibrate, compressing and tensioning the bond (Vincenti and Kruger, 1986:133). For O_2 and N_2, significant vibration begins around 800 K. Finally, when the vibrations become great enough due to the high temperature, the molecules begin to dissociate - O_2 at 2500 K and N_2 at 4000 K – meaning that the following reactions take place (Anderson, 1989:374).

$$O_2 \rightarrow 2O \qquad\qquad N_2 \rightarrow 2N$$

When the temperature reaches 4000 K, the dissociation of oxygen is nearly complete, and the nitrogen dissociation is nearly complete at 9000 K. The first hint of ionization begins between as soon as the dissociation of oxygen begins at 2500 K as the monatomic oxygen combines with diatomic nitrogen to form nitric oxide (*NO*) and monatomic nitrogen. When the nitric oxide forms, some of the molecules immediately begin ionizing into NO^+ and releasing a free electron. The equations by which *NO* forms in air are below.

$$N + O_2 \rightarrow NO + O \quad \text{and} \quad O + N_2 \rightarrow NO + N$$

In cases where a hydrocarbon fuel is burned, additional nitrogen atoms may be emitted causing earlier formation of *NO* and NO^+. Combustion may also cause the formation of

active nitrogen atoms from the nitrogen in air which reacts with the oxygen by the Zeldovich Mechanism to create additional *NO*.

While the fraction of *NO* is small, this is the first temperature at which ions form and there is a chance for detection. When the temperature climbs to 9000 K, both the *O* and the *N* molecules begin to ionize and release free electrons (Anderson, 1989:374). Table 2-2 contain dissociation and ionization temperatures for O_2, N_2, and *NO*.

Temperatures in Kelvin			
Molecule	O_2	N_2	*NO*
Dissociation Begins	2500	4000	-
Dissociation Complete	4000	9000	-
Formation Begins	-	-	2500
Ionization Begins	9000	9000	2500

Table 2-2: Dissociation and Ionization Temperatures in Kelvin (Anderson, 1989:374)

Temperature effects on these chemical reactions are significant and obvious, but changes in pressure also affect the temperatures at which the gases begin to dissociate and ionize. As the pressure falls, the collision rate also falls and the equilibrium point of the dissociation reaction moves to the right of the equilibrium equation causing more atoms to dissociate at lower temperatures. This is a result of the reaction creating two moles of monatomic oxygen and nitrogen from every one mole of diatomic oxygen and nitrogen. When the pressure drops, the gas may expand more easily. It first appears that this characteristic dictates that if the driven side of the tube, which is filled with air, is vacuumed to pressures nearing 0.003 atm, the atoms will more readily dissociate and the temperature needed to dissociate both oxygen and nitrogen to produce NO^+ molecules drops by several hundred degrees. However, when the shock wave propagates through the gas, it also pressurizes it meaning that the reaction happens less readily and the

temperature needed to cause dissociation and ionization actually rises (Anderson, 1989:375).

Although the ideal gas equations in section 2.3 become less accurate at higher temperatures, they can be used to gain a general idea of the Mach numbers needed to raise the temperature to a high enough point to cause dissociation and ion formation. The gas used in the driver side of the tube helps determine the Mach number attainable, but it has no effect on which temperatures can be reached since air is used in each case in the driven section. The equations from section 2.3 were used to determine that when the Mach number reaches 4.2, the theoretical temperature produced by the reflected normal shock is sufficient (2500 K) to begin oxygen dissociation and is roughly the highest Mach number possible in the AFIT shock tube using an air to air system due to vacuum and compressor limitations. Nitrogen begins to dissociate when the Mach number of the incident wave is roughly 5.4 and the temperature from the reflected shock has risen to 4000 K. At the incident wave Mach number of 4.2, the first ions may form from *NO* behind the reflected shock wave. At Mach 6.3, the incident normal shock wave begins to heat the air to temperatures which cause the beginning of oxygen dissociation. At Mach 8.1, the incident shock wave causes the start of nitrogen dissociation and the reflected shock wave heats the air to temperatures near 9000 K causing the beginning of ionization of *O* and *N*. It is important to remember that these Mach numbers are only rough approximations as the equations used to make the predictions are invalidated by the very same dissociation and ionization. CHEMKIN software by *Reaction Design* models the shock tube events using real gas effects and will be used later to determine more accurate predictions of these dissociation and ionization Mach numbers.

The point at which any molecule dissociates or ionizes is determined by the strength of the bond between the atoms and the energy required to break that bond. This energy is called dissociation energy. Molecules with a stronger bond require more energy to separate them. Table 2-3 contains dissociation and ionization energies for selected molecules (physics.nist.gov).

Energies in Kilojoules / mole								
Molecule	O_2	N_2	*O*	*N*	*NO*	*He*	*Ar*	*H*
Dissociation Energy	490.7	942.4	-	-	628.0	-	-	-
Ionization Energy	-	-	1312.6	1403.4	893.8	2373.2	1521.2	1312.6

Table 2-3: Dissociation and Ionization energies of select gases (physics.nist.gov)

The dissociation energy of diatomic oxygen is roughly half the dissociation energy of diatomic nitrogen. This difference is what causes the 1500 K difference between when oxygen begins to dissociate and when nitrogen begins to dissociate. *NO* dissociates at an intermediate energy and, therefore, temperature (Gaydon, 1947:211-212).

First ionization energy is the next important parameter for it predicts when the atoms will ionize and possibly be detected by the sensors. Ionization occurs, in most cases, after dissociation of the diatomic molecule. Therefore, the ionization energies of the monatomic atoms must be examined. The first ionization energy for *O* is only slightly lower than the ionization energy for *N* (Gaydon, 1947:93), (physics.nist.gov). Notice that these energies are considerably higher than the dissociation energies and require a much higher temperature. However, unlike the dissociation energies, the ionization energies are very close to each other indicating that both will begin to ionize around the same temperature. The first molecule to ionize in air is *NO* which has the

lowest ionization energy (Vincenti and Kruger, 1986:165). This ionization begins to occur shortly after O_2 dissociates and allows the formation of *NO*.

The objective of this research is to determine the sensitivity of the ion sensor probes to any ionization caused by a shock wave through air. However, if the objective was to encourage the ionization of the gas inside the shock tube, a promising tactic would be to seed the gas with another gas that would ionize more quickly. In the case of air, adding more *NO* to the mixture would improve chances of ionization at lower temperatures. While it is sometimes useful to use a monatomic gas to produce ions in the shock tube, no gaseous atom in the periodic table has a lower ionization energy than the compound *NO* (physics.nist.gov). Many previous experiments have replaced the air in the driven section of the tube with argon and have typically produced ions behind the reflected shock wave (Tereo and Yamamoto, 1971:43/1),(Schneider and Gronig, 1971:44/1). However, this is unnecessary in this research since the objective is to establish the threshold of detection of the ion sensors in air, not to produce any ions possible.

2.7 Detonations

A great deal of past shock tube research has been dedicated to the study of detonation waves. While it is not the objective of this research to produce or measure a detonation, it is important to understand how one works in order to make proper comparisons between this research and the events in the PDE.

When flammable mixtures are ignited in a tube open at both ends, a flame propagates relatively slowly through the mixture toward the open ends at a speed – on the

order of cm/s – which is dependent on the mixture itself. This wave is referred to as a deflagration wave. When the gas is confined in a small space such as the closed end of a tube, the ignition causes mass motion and turbulence in the gas which increases the speed of the combustion and, under favorable conditions, can develop into an explosive and destructive event known as a detonation with speeds on the order of km/s (Gaydon and Hurle, 1963:257). The most obvious difference between the two forms of combustions is that the flame front of the deflagration wave travels at low subsonic velocities, but the detonation front travels at high supersonic velocities relative to the cold gases in the surroundings (Tucker and others, 2003).

Detonations are essentially made up of two parts: a strong shock front followed by a combustion zone. In a steady detonation, the gas is heated and compressed by the shock front to temperatures which cause spontaneous ignition of the reactants while the heat created by the combustion zone delivers energy back to the shock wave to maintain it (Gaydon and Hurle, 1963:257).

The combustion zone behind the shock wave actually remains subsonic. However, the reason that the combustion zone is subsonic is that the speed of sound is determined largely by temperature. The reactants are subsonic at their heated temperature of several thousand degrees but are supersonic relative to the temperature of the outside air. It is this phenomenon that makes the detonation a powerful source of thrust. When the combustion wave exits the tube, it exits at supersonic, and in some cases hypersonic velocities (Tucker and others, 2003). Figure 2.6 shows a plot of temperature, pressure, and density in a detonation.

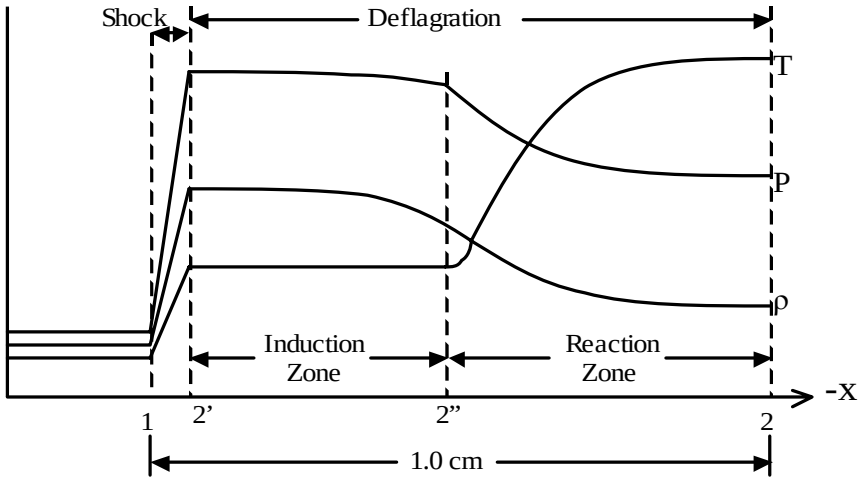

Figure 2-6: P-T-ρ Diagram of Detonation Propagating to the Left (Kuo, 1986:261)

Whether a detonation or a deflagration, the heat of combustion and the chemical reactions in the tube create ions that are detectable by an ion sensor. The sensor measures the presence of combustion when the concentration of ions passing the sensor is high enough that the ions conduct electricity in the circuit. This conduction is denoted by a drop in voltage across a resistor followed by an exponential rise as the sensor recharges. Two sensors spaced apart at a finite length can determine the speed of the wave and the speed can be used to classify the event as a detonation or a deflagration. Another parameter which could be used to determine whether a detonation has occurred is temperature. However, even the fastest response thermocouples available are not fast enough to accurately detect the temperature rise across a detonation wave.

2.8 Pulse Detonation Engines

PDEs are made up of a series of tubes which are cyclically operated to create a near constant source of thrust. The cycle on which the tubes operate is a three stage fill, fire, and purge cycle. The fill stage injects vaporized fuel-air mixture into the tube so that much of the tube is filled with the combustible reactants. In the fire stage, a spark ignites the reactants at the closed end of the tube to begin the combustion process. Depending on the conditions in the tube, this combustion will either propagate down the tube as a deflagration, or it will transition into a detonation. Much of the burned reactants are exhausted out of the open end of the tube, however, to ensure that there are no pockets of burning reactants or unburned reactants in the tube when the fuel valve is opened, a purge valve opens and forces air into the tube to provide a buffer between products and fresh reactants that will be added by the fill stage. As efficiency of the burn process improves, the length of the purge stage can be shortened (Tucker, 2003). Figure 2-7 shows the PDE diagram and cycle.

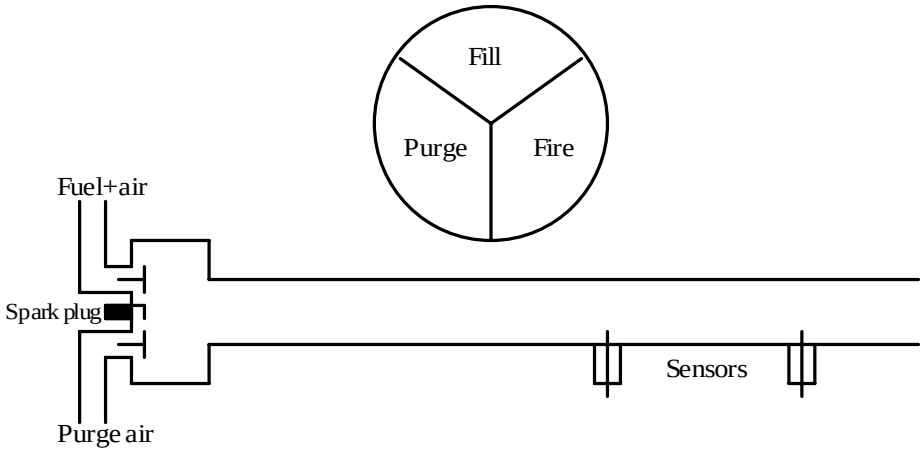

Figure 2-7: PDE Tube and Cycle Diagrams

The thrust produced by the PDE is determined by the velocity and strength with which the combustion and the shock wave exit the open end of the tube. Because the

pressure a detonation is so much higher than that of a deflagration, the thrust and efficiency of the engine is greatly increased. It is one of the current objectives of PDE research to determine exactly what conditions in the tube cause a detonation wave and how to make those conditions reproducible. In order to do this, proper instrumentation is necessary to measure each event. When a detonation wave propagates through the tube, the heat generated is greater that the heat load that an unaltered dynamic piezoelectric pressure sensor can handle. For this reason, the pressure sensors were coated with RTV silicone. However, even with the coating, the sensors are only effective for a short time (Tucker, 2003).

The modified spark plugs used as ion sensors appear to provide the wave speed and are able to withstand high temperatures for extended periods of time. It is unclear whether these ion sensors are detecting ions created by the combustion wave or by the strong shock wave which propagates ahead of it. This research is the first step in ascertaining the true sensitivity of these ion sensors.

As has been previously discussed, this research attempts to detect ions created by a strong shock wave propagating through air. However, in the tubes of the PDE, the shock wave is actually propagating through the vaporized fuel mixed with air. While this research determines whether detectable ions are created by the strong shock wave through air, it will not investigate whether the vaporized fuel is ionized – and therefore detectable by the ion sensors – by the shock wave prior to ignition.

2.9 Chapter Summary

With the gas composition, pressure, and temperature in each section of the shock tube known prior to the burst of the diaphragm, the speed of the shock wave as well as the conditions behind the shock wave can be determined through equations assuming ideal gases, no viscosity, no heat transfer, one dimensional flow, and a perfect diaphragm burst. In addition, the speed of the reflected shock and the conditions behind it can also be calculated. Although these equations provide accurate results up to Mach 3, they are not able to predict real gas effects which may result in chemical reactions and ionization.

Gases other than air may be used in the tube to change the speed of the wave. When lighter gases are used in the driver section, the speed of the shock wave produced is much higher. The higher velocity shock waves heat the gases in the tube to temperatures sufficient to begin dissociating air. The reflected shock causes an added temperature and pressure rise which is even greater than the rise from the incident wave. This wave encourages further dissociation and begins to ionize the air. The first molecule in air to ionize is *NO* and it is therefore the most likely ion to be detected by the sensor.

Detonations create high strength shock waves that have the possibility of ionizing the air-fuel mixture in the PDE prior to combusting it. It is necessary to determine whether the high speed shock waves produced in the controlled environment of the shock tube can cause air alone to ionize at a detectable level for the ion sensors.

3 Materials and Method

3.1 Introduction

This chapter describes the experimental setup used in this research to include shock tube setup, diaphragm selection, sensor locations, shock tube operation, and *CHEMKIN* operation. Error sources are also presented.

3.2 Shock Tube Setup

The AFIT 2-inch shock tube is constructed in 1.52 m (5 ft) sections from type 321 stainless steel tubing (Farnell, 1980:10). The ten 1.52 m sections allow the lengths of the sections to be adjusted to meet the needs of each experiment but at the same time create a limitation in that the length of the tube must be set in multiples of 1.52 m. In this experiment, the driver section was 3.04 m (10 ft) long to reduce the amount of driver gas needed to rupture the diaphragms. The driven section was 4.57 m (15 ft) long in order to obtain a length to diameter ratio of 90 which is within the 40 to 100 range recommended (Gaydon and Hurle, 1963:85). This recommendation is made to ensure that the tube is long enough for the shock to fully develop but short enough so that the attenuation of the shock wave does not become a major factor in the experiment. It would have been ideal to make the tube only one foot longer for the purpose of sensor placement, but there are no short sections available for this tube and adding a 1.52 m (5 ft) section would make the driven section too long to operate with the proper ratio. The inner diameter of the tube is 5.08 cm (2 in.). Both ends of the shock tube are closed to facilitate high pressures in the driver section and a vacuum on the driven section. The shock tube is shown in figure 3-1.

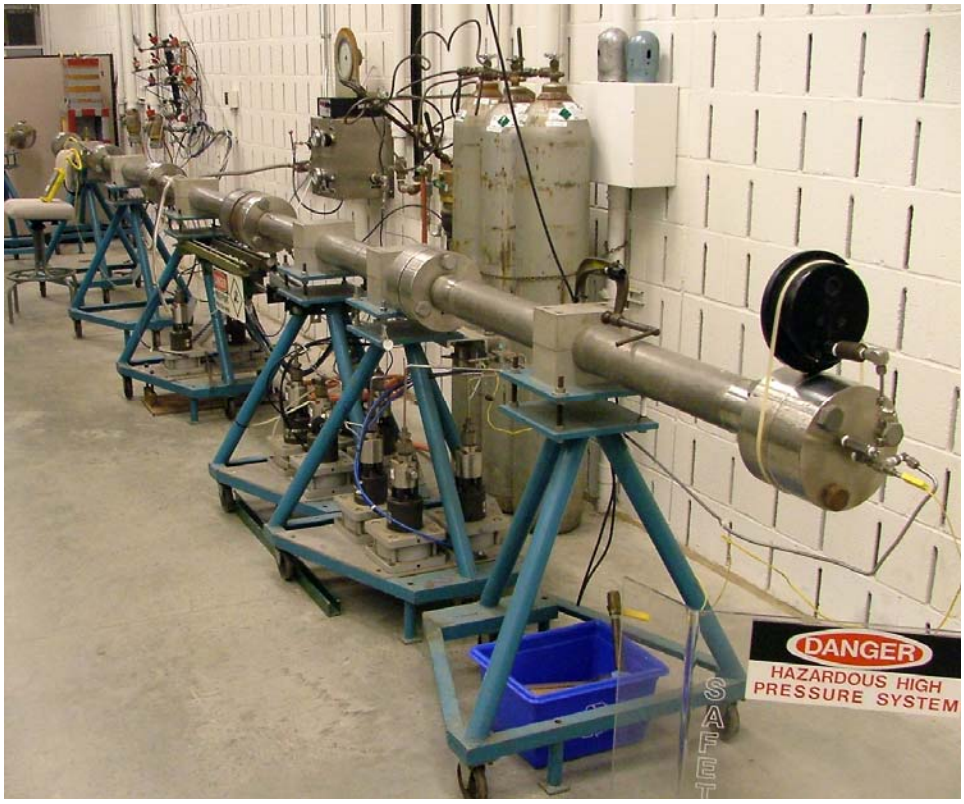

Figure 3-1: AFIT 2-inch Shock Tube

The driver section is connected by quarter-inch steel tubing to a main compressor line. The compressor is rated at 170 atm. A tap was added to the driven section to facilitate the use of a vacuum on the tube. This vacuum is capable of vacuuming the tube down to pressures near 0.003 atm.

3.3 Diaphragms

The shock tube is designed with stations for two diaphragms separated by a void called the double diaphragm section. A high pressure line is tapped in to the space between the two diaphragms from the driver side to allow the double diaphragm section to be set at an intermediate pressure between the driver and driven sections. This intermediate pressure allows for an increase in the total pressure difference between the

two sections. If the pressure between the diaphragms is at an intermediate pressure between the driver and the driven sections, the diaphragms will rupture at a higher pressure ratio (Gaydon and Hurle, 1963:89). While other shock tubes use more predictable means of bursting the diaphragms using magnetic or pneumatic plungers, the diaphragms in the AFIT tube are ruptured only by a difference in pressures. This can lead to large variations in burst pressures if the diaphragms are not identical. Because of the setup of the tube with the double diaphragm section connected to the driver section only, the entire tube can only be vacuumed – this is done when a driver gas other than air is used – when the tube is operating in single diaphragm mode.

Diaphragms of different materials have different characteristic burst pressures. For these experiments, at low pressure differentials, mylar sheets were used. When higher differentials were necessary to achieve higher Mach numbers, stainless steel diaphragms of different thicknesses were used. For very high pressure differentials with full pressure breaking into full vacuum, two stainless steel diaphragms were placed together in one station to achieve double thickness. Each of these metal diaphragms had been etched to allow for a consistent burst. However, due to inconsistencies in manufacturing, the etching on each plate was not identical. As a result, the burst pressure was difficult to predict, and in many cases, the diaphragm did not rupture on both of the axes. When the diaphragm does not rupture on both axes of the etching, the pressure rise and shock wave are slower and the flow is less uniform (Gaydon and Hurle, 1963:90). This makes the speed of the shock wave less predictable as the analytical shock tube equations from section 2.3 assume a perfect diaphragm burst. In some cases, the diaphragms partially petal. That is to say that where four petals should fold up, only two

do. The ideal burst is when all four petals fold up and leave the flow less obstructed. Figure 3-2 shows the various bursts.

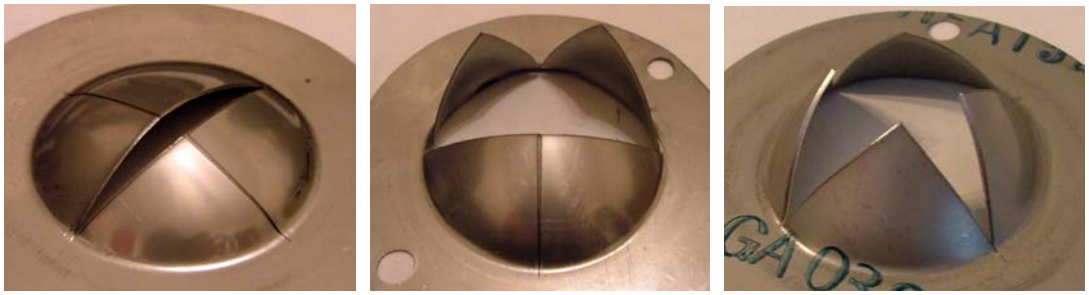

Figure 3-2: Single Axis Burst, Partially Petaled Burst, Fully Petaled Burst (ideal case)

3.4 Sensor Descriptions

In order to determine the pressure in each side of the tube prior to the burst of the diaphragm, an *Endevco* pressure transducer was installed on the driven side of the tube while a *Viatran* transducer was installed on the driver side. On the driven side of the tube, a 1.02 atm (15 psia) sensor was connected to the vacuum lines entering the tube. When the vacuum lines are cut off to prevent the pressure rise from damaging the lines, this sensor is also cut off from the tube. However, the tube held a constant vacuum of 0.004 atm for a full minute in several tests so the change in pressure in the tube before the diaphragm breaks can be assumed to be negligible. On the driver side of the tube, the *Viatran* 137 atm (2000 psig) transducer was installed and used to measure pressure up until the diaphragm broke. This output was measured by a voltmeter. Both transducers were calibrated prior to use in this research.

The pressure sensors used to detect the passage of the shock wave through the tube are unaltered *PCB Piezotronics* ICP® dynamic pressure sensors – Model 102M232. The output from the sensor is passed through 10-32 coaxial cable to a *PCB* Model

402M10 amplifier and then through more coaxial cable to the *PCB* signal conditioner which powered the sensors. The signal conditioner is connected to the data acquisition system. These sensors can measure pressure up to 340 atm in the dynamic range with a resolution of 0.00354 atm. The sensors are designed to operate at continuous temperatures up to 394.3 K (250˚F) and flash temperature up to 1922 K (3000˚F) (*PCB Piezotronics*, 2003).

The dynamic pressure transducers contain a small quartz piezoelectric crystal that emits a charge when compressed. The crystals contain a natural charge which is released when the pressure exerted on them changes. As the pressure holds constant, this charge bleeds off and the output voltage goes to zero. Therefore, these sensors are only useful for detecting changes in pressure. Sustained pressure at any value will eventually lead to a zero voltage output from the sensors. The sensors do, however, emit an extremely fast response to pressure changes which makes them ideal for use in detecting high speed compression waves (*PCB Piezotronics*, 2003).

Sustained temperature in the PDE reaches above 422 K (300˚F) after less than one minute of operation and therefore exceeds the maximum temperature of operation for the pressure transducers. To combat this high temperature problem, RTV silicone is used to coat the end of the transducer. This research must determine whether the RTV detracts from the high speed response of the sensors. Figure 3-3 shows the two sensors with and without RTV. The recession which is filled by the RTV is 0.6 mm deep.

Figure 3-3: PCB Pressure Transducers with and without RTV Silicone coating

The second portion of the research uses ion sensor probes to determine whether the ions caused by the shock wave are detectable. The ions sensors are modified spark plugs which, rather than connecting the circuit by providing a spark for fuel ignition, depend on ions to fill the void where the spark would occur and complete the circuit. When the circuit is complete, the electrode on the probe discharges to ground through the field of ions. The strength of the field determines the rate of discharge. As the field decays with the pressure as the ions recombine with molecules, the rate of discharge decays to zero (Zdenek and Anthenien, 2004:1). The electrical circuit and sample output for the ion sensor is shown in figure 3-4 and the ion sensor itself is pictured in figure 3-5.

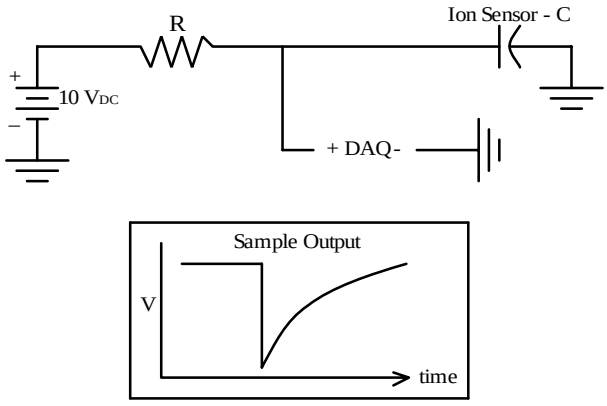

Figure 3-4: Ion Sensor RC Circuit and Sample Output

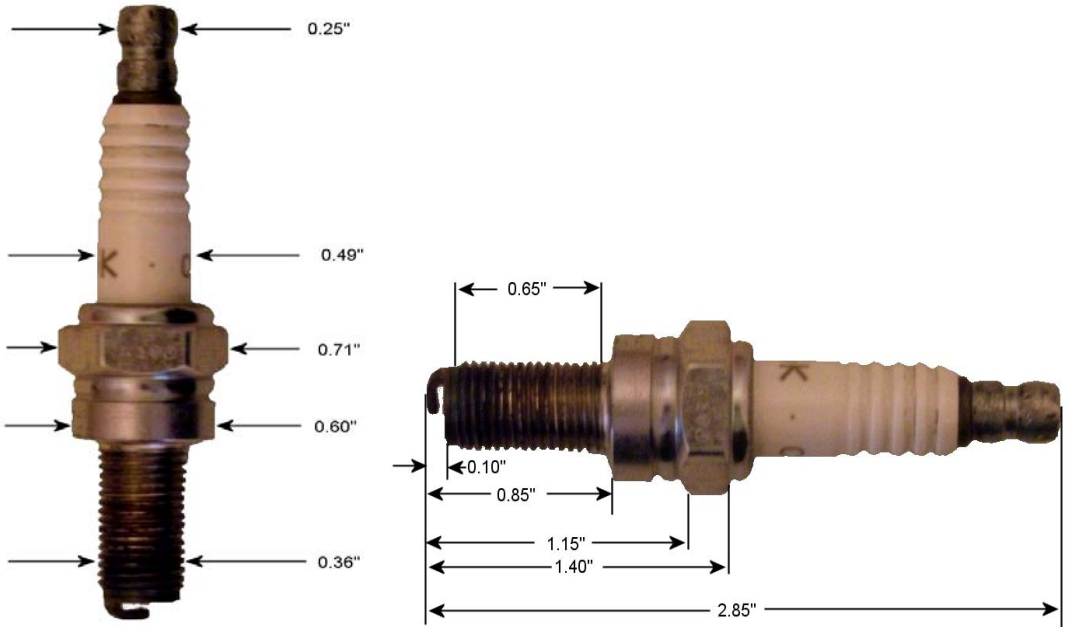

Figure 3-5: Ion Sensor (spark plug) photos with dimensions in inches

Details on all equipment used can be found in Appendix A.

3.5 Sensor Locations

As a check against the experimental results, each run was compared to the analytical solution using the ideal gas equations in section 2.3. Because these equations require temperature, type – K thermocouples were installed on each end of the tube to monitor temperature until the diaphragm broke. The thermocouple on the driver side had a 0.1588 cm (1/16 in.) diameter while the thermocouple on the driven end had a 0.3175 cm (1/8 in.) diameter. The output of both thermocouples was monitored using an *Omega* TrueRMS Supermeter.

In order to determine the speed of each wave, two pairs of dynamic pressure sensors were positioned at two locations in the tube. The first pair of sensors was installed 1.642 meters downstream of the single diaphragm station. The second pair of

sensors was installed 1.511 meters downstream of the first pair of sensors at the end of the five foot section. With a known distance between the two sets of sensors and an experimentally determined time between when the first set detected the shock and when the second set detected the shock, the average speed of the shock wave over that distance can be calculated. For one set of experiments to determine how the shock wave was changing speeds in the tube, a third sensor (*Endevco* 2000 psig) was installed 1.556 meters downstream of the second sensor. Figure 3.6 is a diagram of the locations of the sensors in the tube.

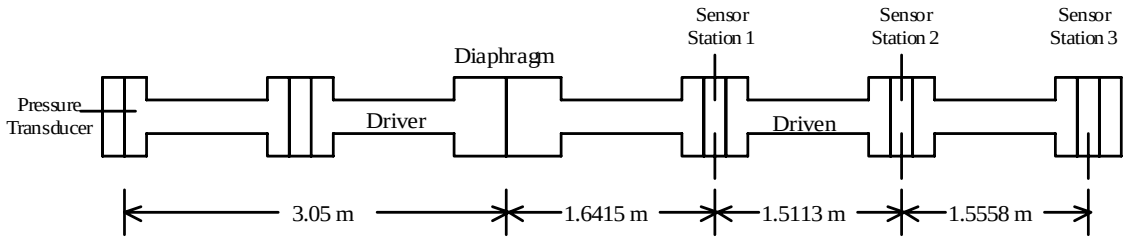

Figure 3-6: Diagram of tube and sensor locations

In an experiment which compares the response of two sensors at one location, it is critical to know exactly where each sensor is in relation to the other. In this experiment, the sensors were installed in plates which join sections of tube together. Due to machining errors, one sensor in the first pair was located 1.25 mm before the second sensor in the pair along the length of the tube. The second set of sensors were only 0.20 mm apart along the length of the tube. While small, these differences cause shifts in the data between the two sensors which are visible when the data is taken at a high enough rate. The offset between sensors at the first location did impact the results of this experiment.

Due to the unsteady flow immediately exiting the driver section through the burst diaphragm, it is desirable to have the sensors as far downstream from the diaphragm as possible. As Mach number rises, the distance needed for the shock wave to reach peak velocity is greater. In this experiment, the peak shock velocity is less than Mach 9. For this Mach number, the peak shock velocity is not achieved until the shock has reached the second set of sensors (Gaydon and Hurle, 1963:80). The length of the driven section was limited to 4.57 m (15 ft) as previously discussed and the possible sensor locations at the end of the tube were within one centimeter of the end of the tube. Because of the interaction of the reflected shock wave on this sensor, it was determined that the sensors should be placed at the other two locations in the driven section. The ideal situation would have been to add a small 0.25 m section onto the end of the tube but such a section was unavailable. The assumption was that any unsteady flow after 1.5 meters would not be sufficient to detract from the data and detecting both the incident and reflected shock waves was more important.

After determining the effect of RTV on the sensitivity of the dynamic pressure transducers, a single pressure transducer was removed from each location and replaced by an ion sensor probe. The two remaining pressure sensors are used to determine the average wave speed and to confirm the presence of a shock. The ion sensors are used to attempt to detect ions created by the shock wave. In this way, the sensitivity of the ion sensors can be determined.

The sensors were installed in plates which join sections of the shock tube. Ports were installed in the plates and manufacturing inaccuracies caused the sensors to protrude into the tube as shown in figure 3-7.

Figure 3-7: *PCB* Transducer protruding into shock tube

Despite this manufacturing flaw, the impact on the measurement should be minimal. The protruding transducer casing will likely cause oblique shocks as the shock wave passes but the measurement should still be the result of the normal shock wave. The normal shock wave will also reach the next set of sensor prior to the oblique shocks ensuring that the measurement on those sensors is also the result of the normal shock wave. The disruption in the flow will likely weaken the normal shock wave but not to the extent that the results will be severely affected.

3.6 Gas Selection

In comparing the dynamic pressure transducers with RTV silicone coating to the transducers with no coating, hypersonic shock waves are not necessary. A range of shock waves between Mach 1.5 and Mach 4 can be produced without the use of gases other than air. For this reason, air was used on both sides of the shock tube for this set of tests with the vacuum used for the higher Mach numbers.

In order to achieve Mach numbers which heat the air to temperatures causing dissociation and ionization as discussed in section 2.6, it is necessary to use gases other

than air as discussed in section 2.5. In this research, helium was chosen as the driver gas to achieve shock speeds near Mach 8 and avoid the possible combustion caused by hypersonic hydrogen penetrating air. Three helium tanks containing 8.50 cubic meters of helium pressurized to 150 atm were connected to a single manifold used to tap into the high pressure air lines before reaching the regulator. In this way, the gas provided by the bottle farm is regulated by the same regulator as the air. Two manual 90˚ valves isolate the helium bottle farm from the high pressure air supply.

3.7 Shock Tube Operation

The shock tube is controlled by manual valves, solenoids, and pneumatically driven valves. A manual valve isolates the 6.8 atm (100 psi) shop air from the rest of the system. When open, this air charges all the lines up to the manifold of solenoids. These solenoids are operated from a control panel (shown in figure 3-8) in the control room and control the flow of air to the pneumatic valves. The pneumatically operated valves all fail in the closed position for safety purposes. Most manual valves are safety backup valves for the remotely operated pneumatic valves.

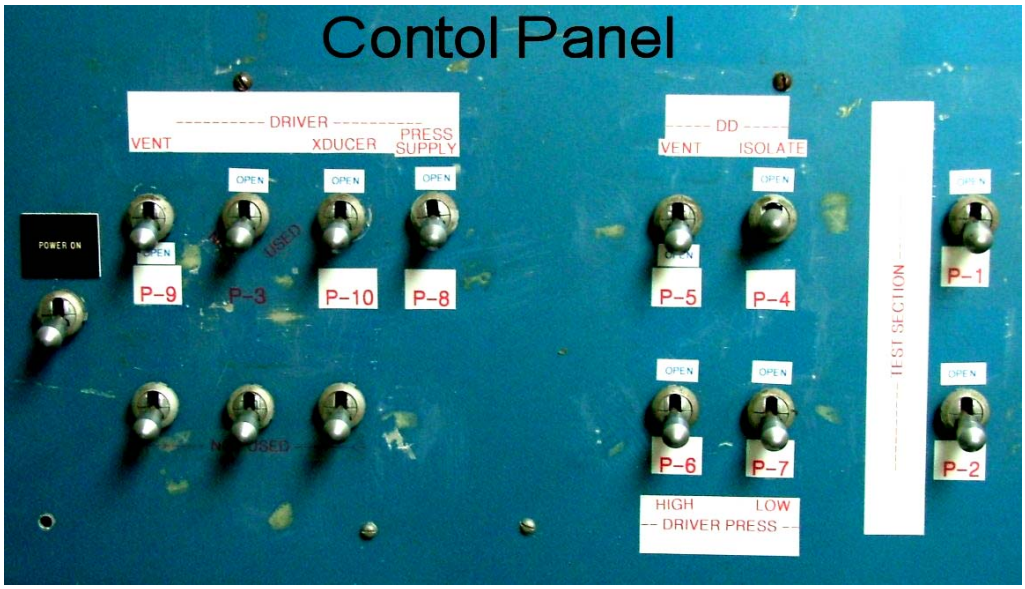

Figure 3-8: Shock Tube Control Panel

A single solenoid followed by a manual 90˚ valve (shown in Figure 3-9) are separate from the rest of the system and control the flow of the high pressure air from the regulator to the tube. In addition, two pneumatic valves offer extra safety checks between the regulator and the tube.

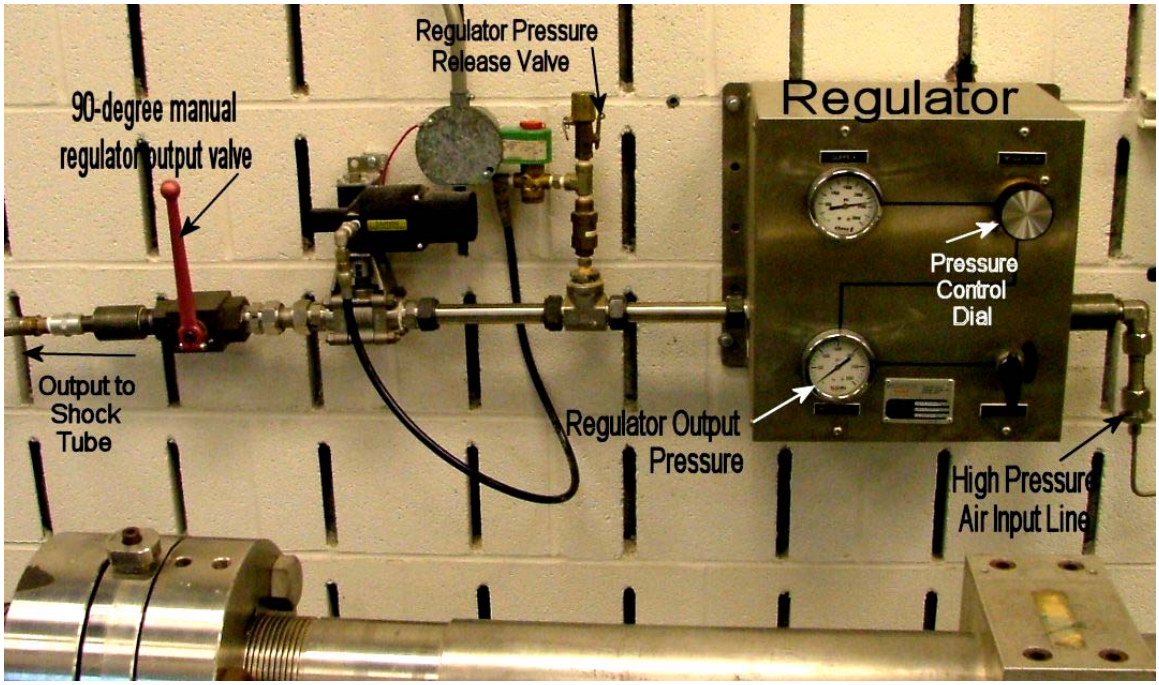

Figure 3-9: High Pressure System

Pneumatic valves operate vents in each section of the tube to bleed the pressure to atmospheric pressure. The vacuum line utilizes 6.8 atm (100 psi) tubing and therefore cannot be left exposed to high pressures. It is protected behind a manual valve and a pneumatic valve. The vacuum gage is also connected to the same 6.8 atm tubing and is cut off from the remainder of the tube during operation as well.

The full detailed procedures for all operations on the shock tube including the changing of diaphragms can be found in Appendix B. The diagram of the piping for the shock tube is also included in Appendix B.

3.8 Data Acquisition System and Operation

The data acquisition board is a *National Instruments* PCI-6110 board connected to an NI-BNC-2120 input box. The data is read by a program called Online Wave Speed

which was developed by Jeff Stutrud of the AFRL Propulsion Directorate, Turbine Engine Division, Combustion Sciences Branch specifically for high speed data acquisition in the pulse detonation engine. The program runs on top of *LabVIEW 7* software. A modification to the program for shock tube research is a threshold trigger to capture the shock wave. When the data spikes above the set threshold for that test, the data in that one-second block is sent to the bottom screen and the data can be saved. When saved, the data can be analyzed using the PT Reader software also developed at AFRL. The procedures for operating both Online Wave Speed and PT Reader in addition to the checklist for completing shock tube experiments can be found in Appendix C.

3.9 Modeling – CHEMKIN

The 'Shock Application' of the software CHEMKIN was used to simulate shock waves between Mach 5 and Mach 8.5 to predicts temperatures, pressures, and the dissociation of air behind both the incident and reflected shock waves. Wave speeds as low as Mach 1.25 were used to predict the speed of the reflected shock wave as well. CHEMKIN utilizes real gas effects including viscosity to predict the conditions inside the shock tube after each wave. It also uses gas chemistry files which include the chemical reactions which occur in air at high temperatures in order to determine dissociation and ionization in the air. In doing so, it provides a comparison to the analytical, ideal gas solution and allows the experiments to be tailored to achieve certain Mach numbers and dissociations. CHEMKIN requires the input of the initial pressure and temperature in the driven section as well as the velocity of the incident shock wave.

CHEMKIN also makes assumptions of the events in the shock tube as it does not take into account heat transfer to the surrounding tube, unsteady flow from the diaphragm burst, and, in the reflected case, viscous effects. Therefore, while more accurate than the ideal gas solution, the CHEMKIN results should only be used as a guide for shock tube performance and should not be expected to perfectly predict the events.

3.10 Error Analysis

The results presented in this experiment are subject to various forms of error due to data system limitations as well as variations in the setup. The data acquisition system recorded data at 2 MS/s and was trimmed to 1 MS/s for data analysis to create a manageable file size. At 1 MS/s, a data point was recorded at 1μs intervals giving each data point a ±0.5μs error. The rise times of most shock waves in these experiments were on the order of 8μs and are therefore not significantly affected by the difference in temporal resolution when the acquisition rate is reduced from 2 MS/s to 1 MS/s.

The positions of the sensors at each station relative to the next station is accurate only to 2 mm giving an error of ±1 mm. The pressure transducers have a face that is 5 mm in diameter. It is impossible to determine whether the sensors detect the wave at the leading edge, trailing edge, or center of the sensor creating a ±2.5 mm error. The ion sensors have a range of detection of 1.3 mm making an error of ±0.65 mm. The total position error for the pressure transducers is ±3.5 mm while the ion sensor position error is ±1.65 mm.

The digitization of the data adds to the error as the data acquisition system records voltages in steps of 0.98 mV for the pressure transducers and 2.4 mV for the ion sensors.

The subsequent error for the pressure transducers and the ion sensors is ±0.49 mV and ±1.2 mV respectively (NI-6110 Manual)

The pressure transducers used in these experiments have various resolutions as do the ion sensors. Table 3-1 shows the error of each transducer and ion sensor in millivolts and atmospheres.

Serial No.	Error (mV)	Error (atm)
15010	±0.836	±0.0567
15008	±1.033	±0.0748
18000	±0.638	±0.0408
17993	±0.964	±0.0646
ion 1	±25.0	N/A
ion 2	±25.0	N/A

Table 3-1: Sensor Resolution

While quantitative values for other sources of error cannot be determined, these sources must be considered in evaluation of the data. Calibration errors in all pressure sensors contribute to the uncertainty in the pressure measurements. The pressure of the high pressure driver section was manually read from a voltmeter. Leading up to the burst of the diaphragm, the pressure was constantly changing and the voltmeter could only output an average voltage over the last 0.25 seconds. When the burst of the diaphragm was heard, the current value on the display was recorded.

Gas dilution contributes to the error as well. Before each run using helium, the entire tube was vacuumed to less than 0.005 atm before being filled with helium. While the amount of air remaining in the mixture is small, it may affect the results by slightly slowing the wave speed. After each run, the tube was not completely flushed with air to expel all helium before conducting the next test. Helium remaining in the driven section could skew the results by encouraging a faster wave speed but a lower temperature rise

across the shock. Future experiments should be sure to use high pressure air to force all helium from the tube.

3.11 Chapter Summary

The AFIT 2-inch shock tube is assembled from multiple 1.52 m sections to create driver and driven sections of desired lengths. In this research, the driver section was set at 3.04 m and the driven section length was set at 4.56 m. Instruments can most easily be installed through ports in the plates which join each section. All three joints in the driven section accommodate sensors. *PCB* piezoelectric dynamic pressure transducers are used in these experiments and are coated with RTV silicone to determine its effect on the effectiveness of the transducers. Ion sensor probes are also used to determine whether shock waves in air create enough ions to complete the circuit of the sensor and be detected. All operating procedures can be found in Appendix B and C.

4 Results and Analysis

4.1 Introduction

This chapter describes the results of calculations using the analytical shock tube equations from section 2.3 and the results of shock modeling using CHEMKIN. The results of tests examining the effect of an RTV silicone coating on pressure transducers are presented along with results of testing on the sensitivity of an ion sensor probe. Finally, all results are compared and an analysis of the performance of the AFIT shock tube is given.

4.2 Analytical Solution – Ideal Gas Assumptions

To improve the efficiency of the research, prior to testing, the analytical shock tube equations from section 2.3 were used to develop predictions for necessary pressure ratios to achieve certain Mach numbers and what temperature effects those Mach numbers would provide. All calculations were performed assuming that the temperature in both the driver and the driven section of the shock tube was 294.26 K (70˚F). The result was a series of plots that can be used to configure each test. Tables in Appendix C show the calculated values for pressure ratio and temperature ratio within the limits of the AFIT shock tube. Figure 4-1 shows the pressure ratio needed to achieve a desired Mach number in experiments with air as the driven gas and either air or helium as the driver gas.

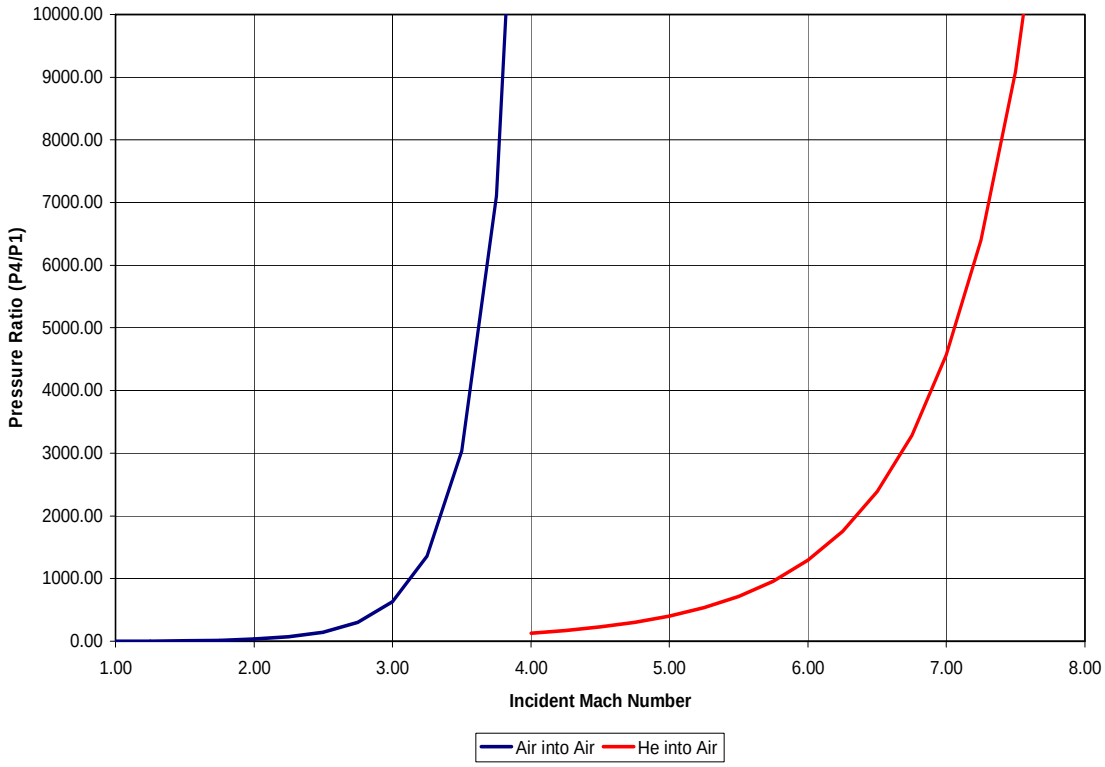

Figure 4-1: Necessary Pressure Ratio to Achieve a Given Mach Number (Analytical)

The temperature ratios that are calculated using the analytical equations are independent of the initial temperature, the initial pressure, and the gases used. The temperature ratios depend only on the incident shock Mach number. Figure 4-2 shows the temperature ratios resulting from various Mach numbers. (Recall that T2/T1 is the ratio of temperatures across the incident shock wave, T5/T2 is the ratio of temperatures across the reflected shock wave, and T5/T1 is the ratio of the temperature behind the reflected shock to the temperature in front of the incident shock.)

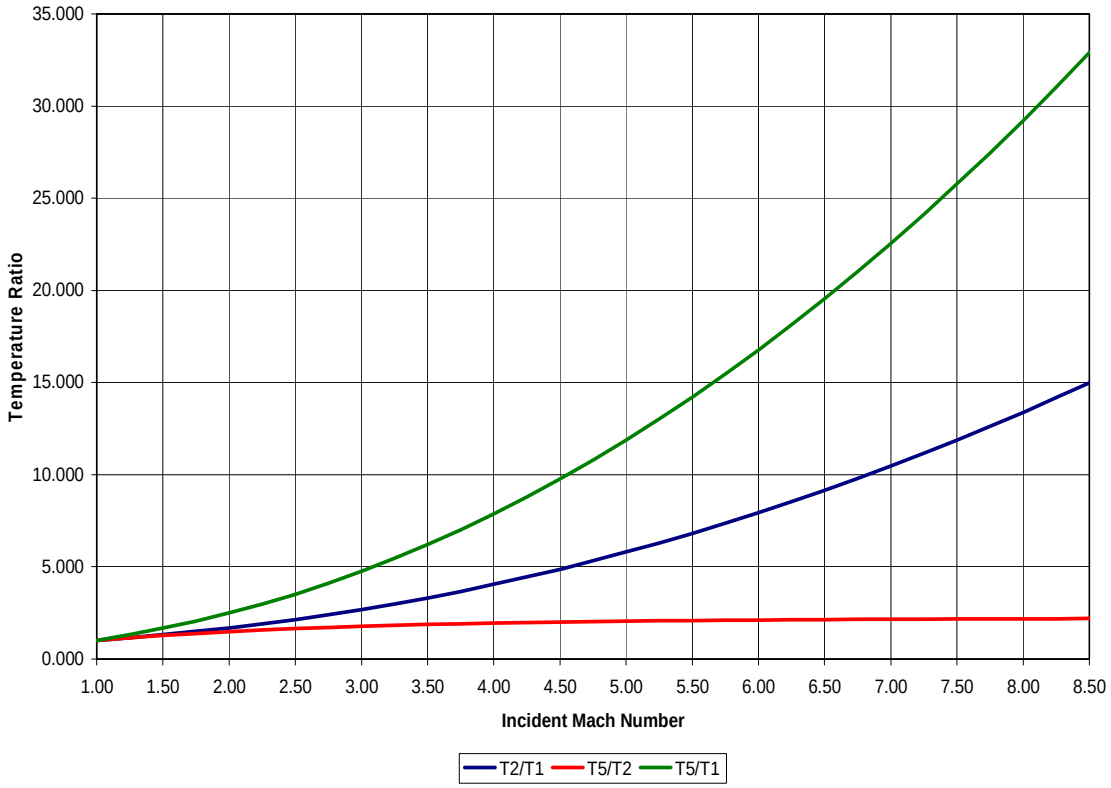

Figure 4-2: Temperature ratios resulting from various Mach numbers (Analytical)

The final parameter calculated using the analytical solution was the Mach number of the reflected shock wave. Like the temperature ratios, it is only a function of the incident shock Mach number. Figure 4-3 shows the reflected shock Mach number versus the incident shock Mach number.

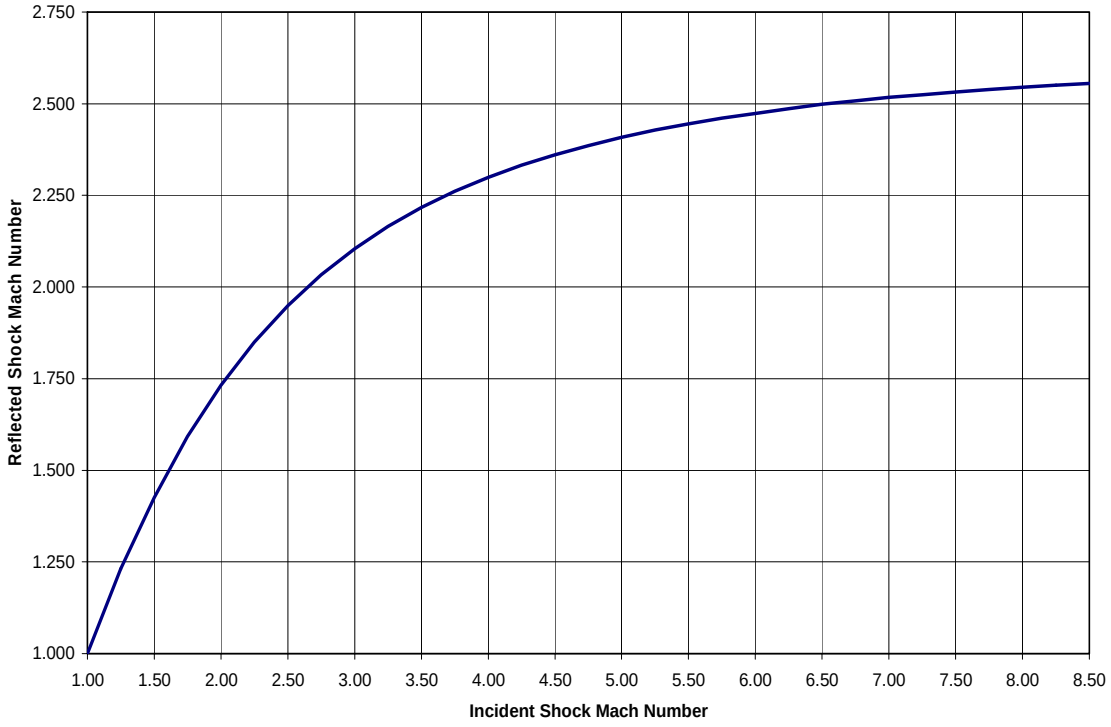

Figure 4-3: Reflected Shock Mach Number vs. Incident Shock Mach Number (Analytical)

4.3 Shock Modeling in "CHEMKIN" – Real Gas Effects

CHEMKIN runs were conducted for a range of shocks with three different driven section initial pressures: 0.003401 atm (0.05 psi), 0.00851 atm (0.125 psi), and 0.01361 atm (0.20 psi). In all cases, the initial temperature of the driven section was taken to be 294.26 K (70˚F). For a boundary layer correction, the viscosity was entered as 1.777 E-4 g/(cm-s). The composition of air was entered in mole fraction for N_2, O_2, and Ar as 0.78118, 0.20948, and 0.00934 respectively. The shock speed was varied from Mach 5 to Mach 7 in steps of Mach 0.5 analyzing the reflected shock only and varied from Mach 7 to Mach 8.5 in steps of Mach 0.25 analyzing both the incident and reflected shock. These parameters were selected based on the temperatures created by these shock waves. Air does not dissociate for the reflected shock below Mach 5 and for the incident shock

below about Mach 6.8. Dissociation levels slowly increase as the temperatures get higher from faster shock waves. The AFIT shock tube is not capable of producing a wave speed higher than Mach 8.5 under the current setup.

For each run, the CHEMKIN-calculated pressure and temperature behind the shock wave were recorded along with the molar concentration (mole/cc) of monatomic nitrogen, monatomic oxygen, and nitric oxide in order to determine levels of dissociation. Figure 4-4 and figure 4-5 show the pressure and temperature respectively behind both the reflected shock and the incident shock as a function of incident shock Mach number. While the pressure varies according to the initial pressure (based on ratios), the temperature effect is negligible, and therefore, the temperature curve for only one of the initial pressures is shown.

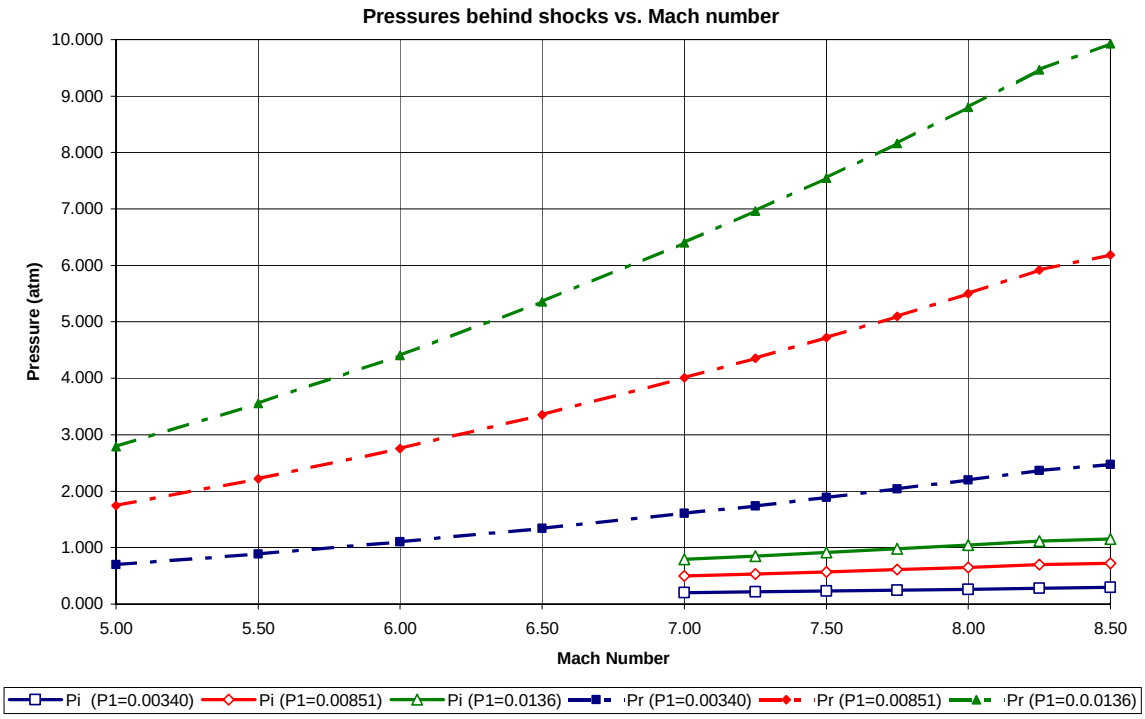

Figure 4-4: *CHEMKIN* generated plot of pressures behind incident and reflected shocks given initial pressures in parenthesis

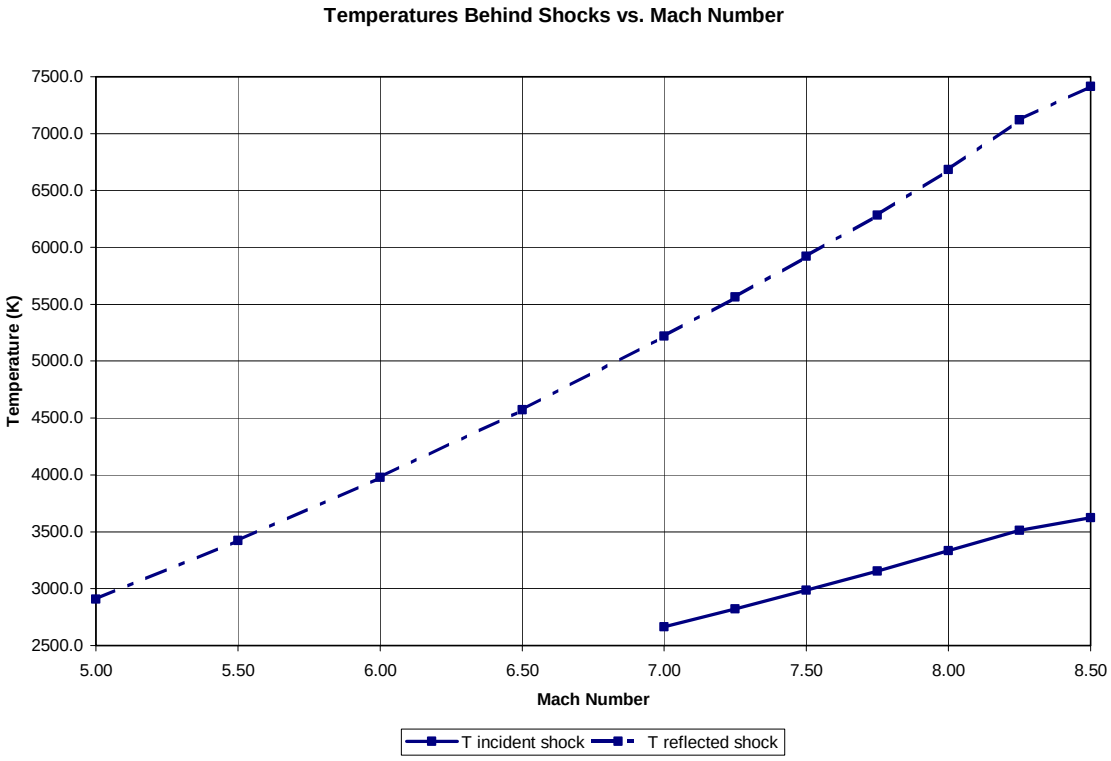

Figure 4-5: *CHEMKIN* generated plot of the temperature behind incident and reflected shocks

The molar concentration of monatomic oxygen, monatomic nitrogen, and nitric oxide was also recorded for each Mach number tested. In the case of the incident shock, because the gas has yet to be heated, a much higher speed shock wave is needed to induce dissociation. The reflected shock wave uses the gas preheated by the initial shock wave to raise the temperature further and induce dissociation and ionization. Figure 4-6 shows the molar concentrations in mole/cc for the incident shock wave while figure 4-7 shows that of the reflected shock wave.

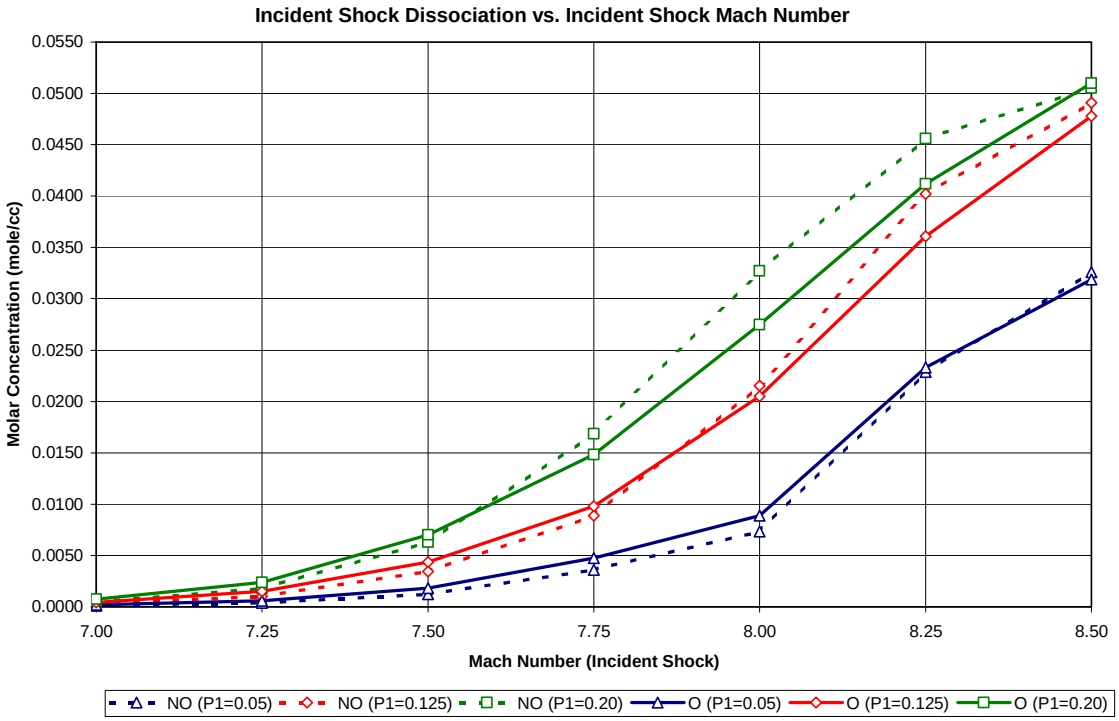

Figure 4-6: *CHEMKIN* generated plot of dissociation due to the incident shock wave

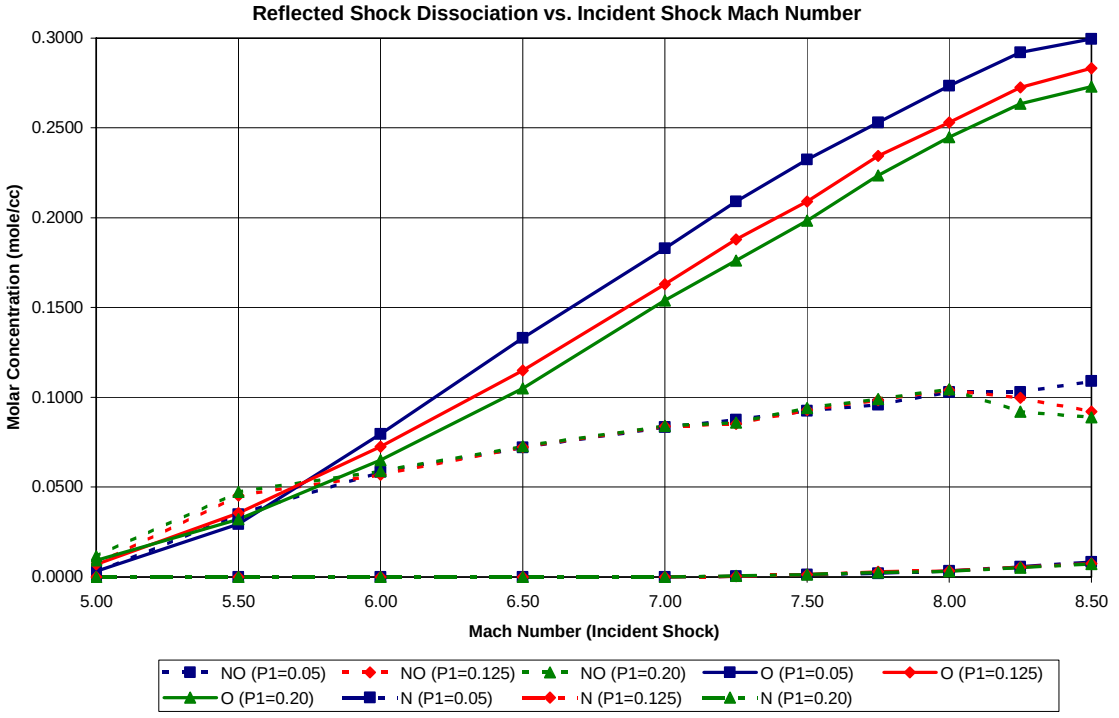

Figure 4-7: *CHEMKIN* generated plot of dissociation due to the reflected shock wave

4.4 Pressure Transducer Variations

Prior to running tests to compare the response of pressure transducers with an RTV silicone coating to those without a coating, experiments were performed to verify that all the transducers being used were exhibiting the same dynamic responses. Tests were conducted by observing the response of the transducers to the changes of state in the tube from pressurizing to venting over a 13 second time period. The results of the tests showed that while most transducers exhibit similar responses – within 5% on large pressure changes – some transducers vary from this norm by displaying either lower pressures or pressure jumps. Extensive troubleshooting was conducted that determined that the sensors were the cause of the erroneous readings.

All transducers tested responded with spikes of numerically equal magnitude when the state of the tube changed (i.e. a valve was closed or opened). Of the initial four transducers installed, three displayed a nearly identical pressure rise while the fourth transducer showed a value that became progressively further from the other three. The three which performed with consistently matching outputs provide data that correlates closely to the pressure change as displayed by the differential transducers providing readings in psig. It is significant that the transducer which exhibited the fast discharge still shows spikes when there is a change of state in the tube because this indicates that the response is neither slow nor weak. It also disproves the possibility that the amplifier is not functioning properly. The most logical explanation is that the charge bleeds off too quickly and prevents an accurate reading when there is a steady rise or fall in pressure. This response could be caused by use and abuse in heated conditions of the PDE since the transducer had been used before. It could also be the result of applying too much

torque when installing into a tube since this can deform the casing. The torque on the sensor was adjusted in the tests and produced no difference in the results. The sensors were not intentionally over-tightened, but if this happened at a previous instance, it may have a lasting effect. Figure 4.8 shows the response of the original three sensors to pressure increases and decreases in the tube.

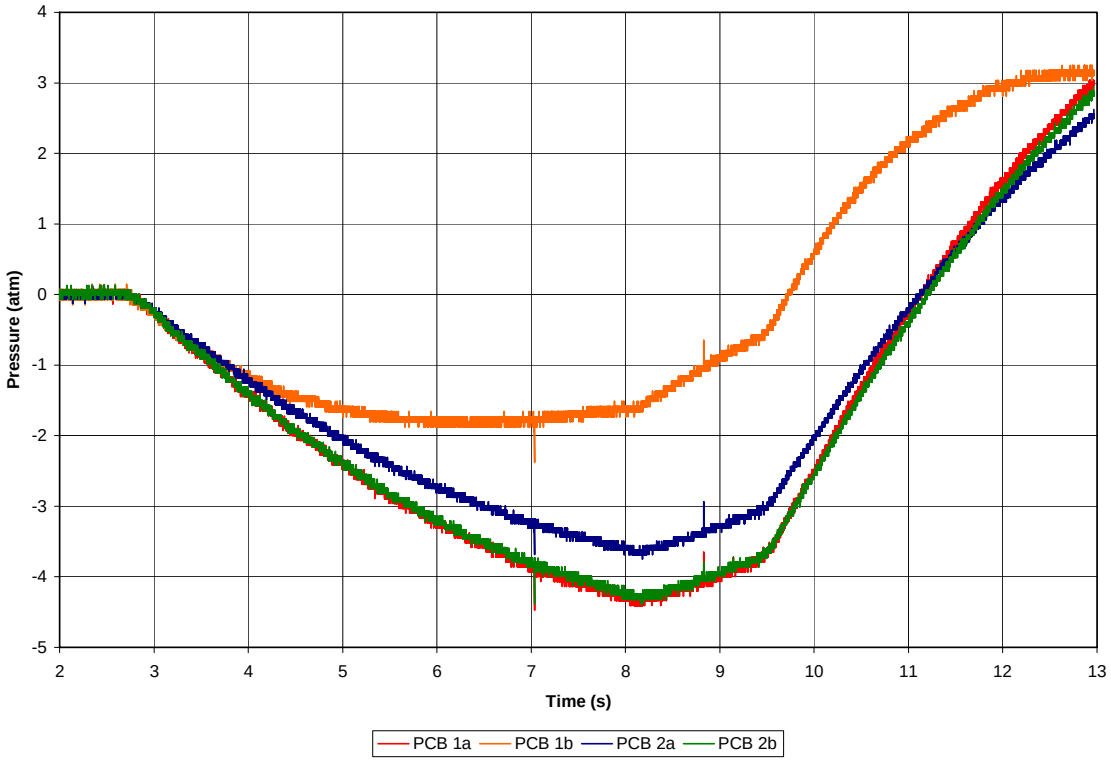

Figure 4-8: Experimental sample of fast discharge of sensor in response to pressure changes (sensor shown in orange not used in testing)

Four additional transducers were tested individually against the three which showed excellent agreement in the first tests. Of the four additional transducers tested, two exhibited the same rapid discharge as the original transducer. One performed inconsistently giving good readings on two tests, lower readings on one test, and no response on two tests. The final transducer showed excellent agreement with the original

three transducers and was selected for use in the remainder of the research. Table 4-1 displays the serial numbers of the transducers which exhibited the various responses.

Characteristic	Serial Numbers
Good Response	15008, 15010, 17993, 18000
Fast Discharge	15004, 15005, 15007
Erratic	15009

Table 4-1: Transducer Serial Numbers and Response Characteristics

Several other conditions can cause erroneous readings or instability in the output. The connecting cables use fiber-optics and cannot be bent at sharp angles. This could be reason for many jumps in pressure and instability at steady state. Certain transducers including number 15009 occasionally reset themselves to zero in the middle of a test. The cause of this phenomenon was not determined as the transducer stopped providing any output after only three tests. Occasionally all sensor readings will begin to show instability and jump around while at a steady state atmospheric pressure. This can be solved by turning off the signal conditioner for five minutes and letting the transducers cool. Ensure all connections are secure while the conditioner is off, and then turn it back on and the readings should return to normal.

4.5 RTV Silicone Effects on Transducer Output

A series of tests were performed at different Mach numbers to test the four *PCB* transducers with and without RTV silicone. Fifteen tests were conducted using all four sensors without RTV silicone at Mach numbers ranging from 1.71 to 3.60. In all tests, the transducers exhibited similar responses with changes resulting from different pressure ratios. The two sensors at station 1 consistently showed sensor 1a trailing sensor 1b by 2 μs (±0.5 μs) in sensing the pressure spike of the shock wave. The two sensors were

found to be offset by 1.25 mm inside the tube. The speed of the shock waves varied from 589 m/s to 756 m/s with the waves traversing this 1.25 mm gap in 2.12 μs to 1.65 μs respectively. The time gap between the detection of the wave between the sensors varied according to wave speed with the larger time gap occurring on slower waves. The remaining variation in this delay time gap beyond that which can be explained by the spatial gap falls within the error inherent in the experimental measurements. Therefore, sensors 1a and 1b detected the shock wave at statistically the same time. Sensors 2a and 2b located at station 2 were separated by only 0.2 mm and showed no visible variation in the time at which the shock wave was detected.

Figures 4-9 and 4-10 show the pressure response of the sensors to the shock wave without an RTV coating. Figure 4-11 is the same as Figure 4-9 with a correction factor applied for the 1.25 mm of spatial variation between the sensors. The pressure ratio at which the shock occurred is in parentheses. Error bars on the plot show the error due to the data acquisition system. While position errors also existed, the errors are only pertinent when determining the time delay from one set of sensors to the second for a wave speed calculation. For wave speeds of 600 m/s, this position measurement error amounts to only a 1 m/s error.

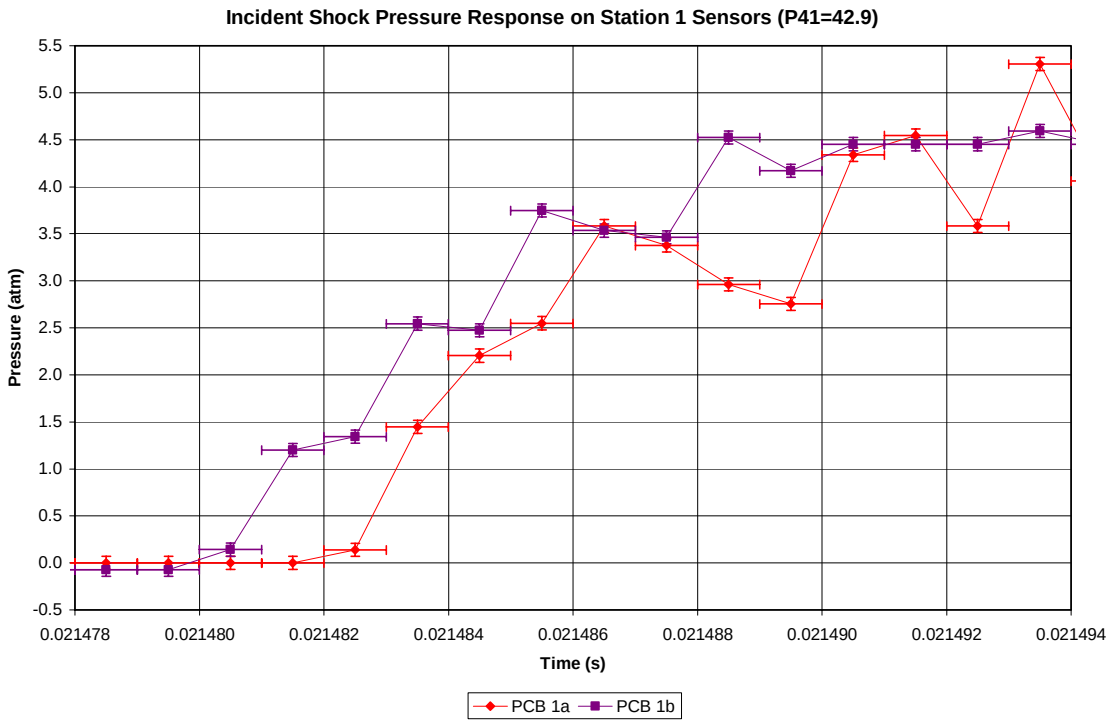

Figure 4-9: Pressure response in atm of station 1 sensors with no RTV

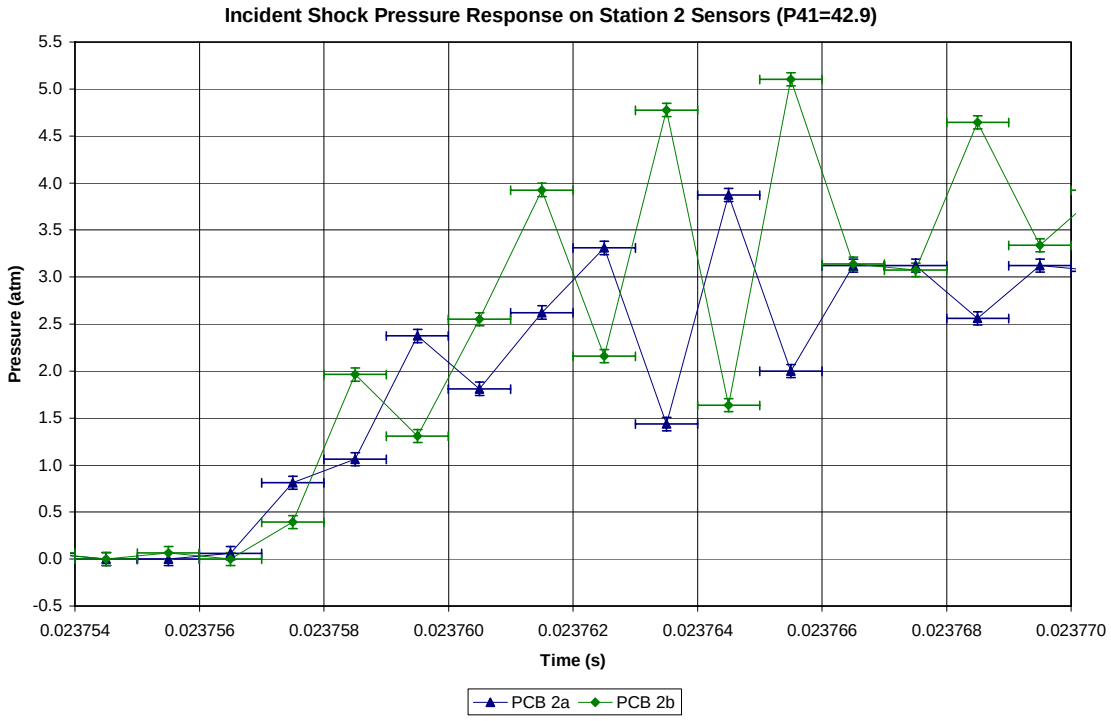

Figure 4-10: Pressure response in atm of station 2 sensors with no RTV

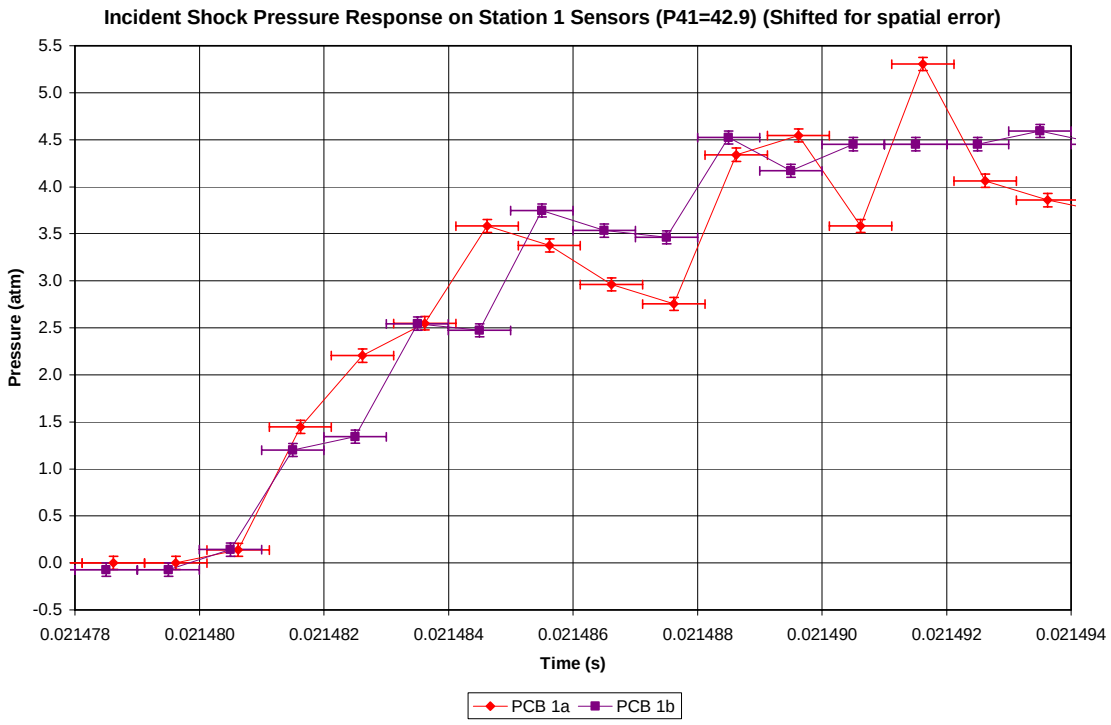

Figure 4-11: Pressure response of station 1 sensors with no RTV (corrected for 1.25 mm gap)

The peak pressures of the spike displayed by sensors are also the same showing that the sensors have nearly identical responses without RTV coatings on any of them. Because of this similarity, it can then be stated that after RTV is applied, any change in sensors 1b and 2b in relation to sensors 1a and 2a respectively is due to the effects of the RTV silicone coating. Twelve tests were completed adding an RTV silicone coating to one of the two sensors at each station. Figures 4-12 and 4-13 show the sensor responses with RTV silicone applied (0.6 mm thick to fill recess in sensor) to sensors 1b and 2b. Figure 4-14 is the same as Figure 4-12 with a correction factor applied for the 1.25 mm of spatial variation between the sensors.

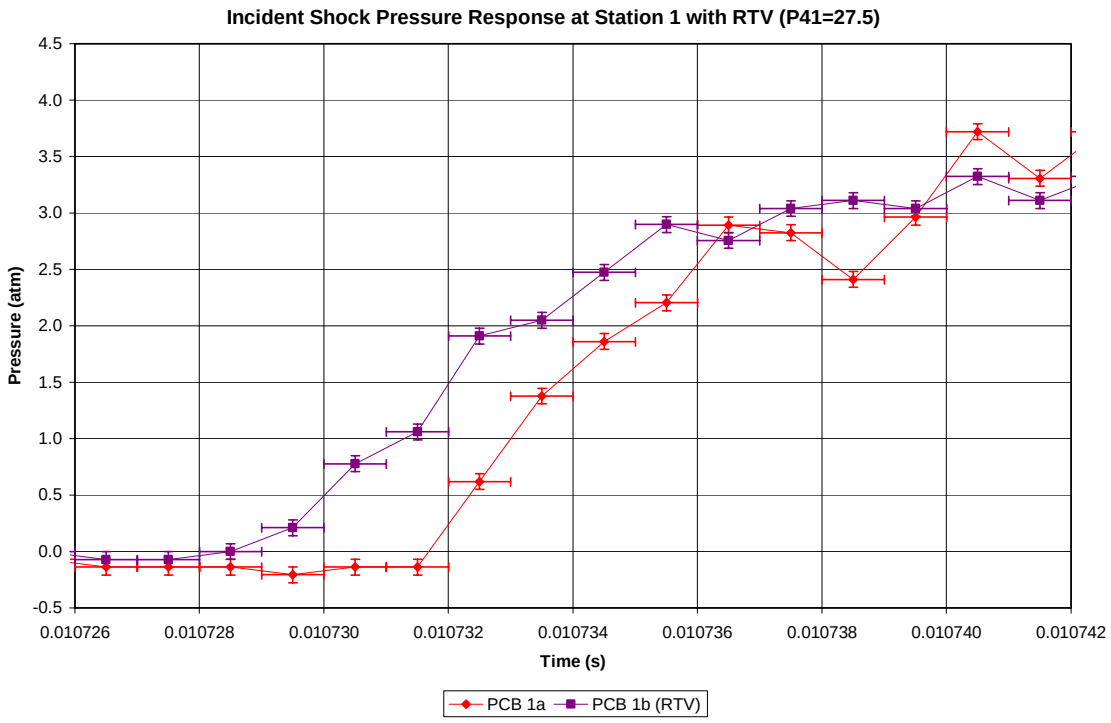

Figure 4-12: Pressure response in atm of station 1 sensors with RTV

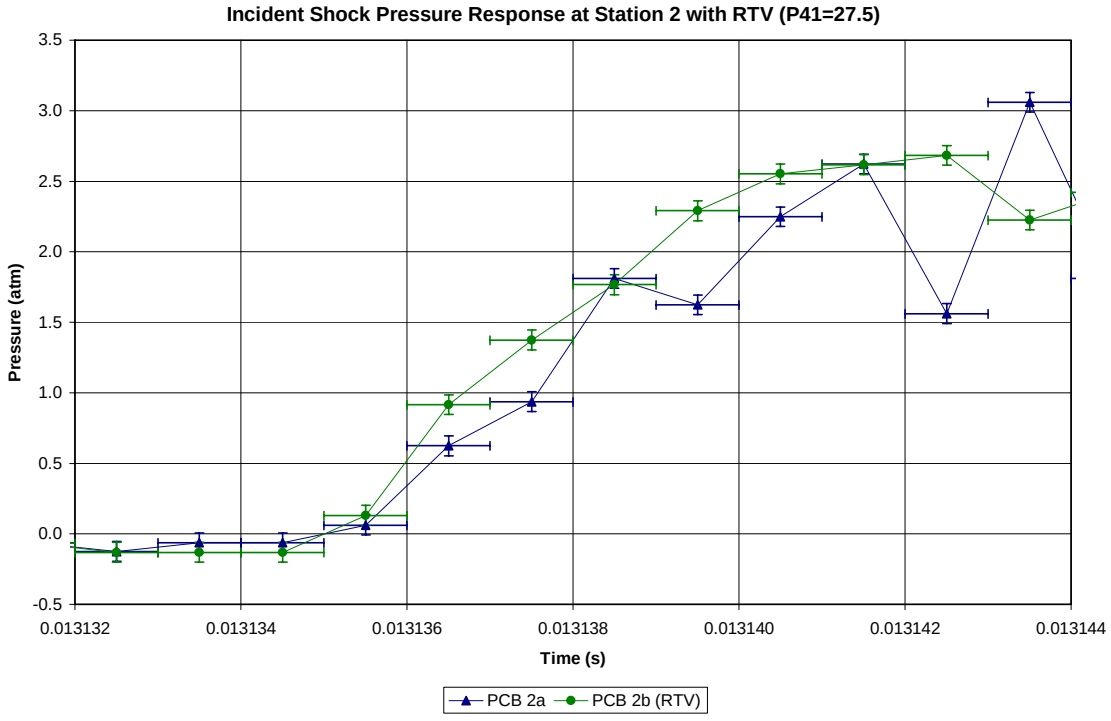

Figure 4-13: Pressure response in atm of station 2 sensors with RTV

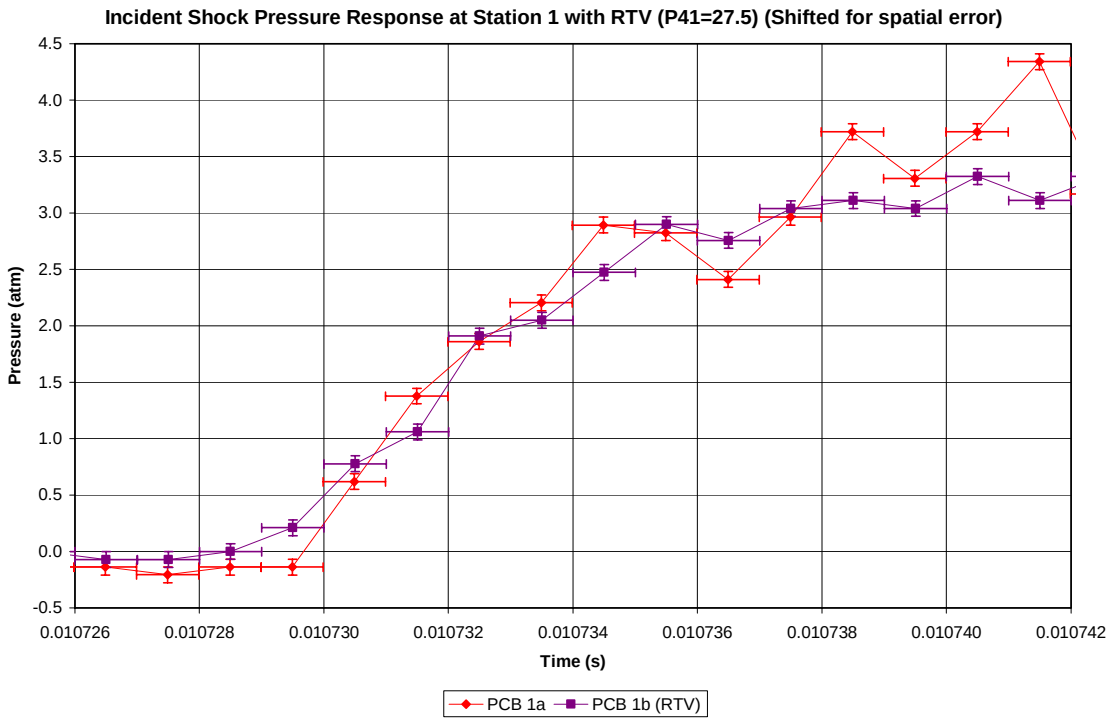

Figure 4-14: Pressure response in atm of station 1 sensors with RTV (corrected for 1.25 mm gap)

Figure 4-12 shows the sensors at station 1 exhibit the same delay as was observed in the plot without RTV silicone. Because this delay is an effect of the spatial difference between the two sensors as shown in Figure 4-14, it can be stated that the sensor responses are statistically the same. One change that can be seen between the plots with and without RTV is that the data points when RTV has been applied are much more stable with fewer spikes and drops from one data point to the next. The peak pressure of the spike at station 1 shows that the sensor with the RTV coating displayed a lower value by 0.5 atm. However, this is not the case with the sensors at station 2 as the peak pressure was identical within the error and the noise in the data. Like station 1, the sensors at station 2 show an identical response and rise time with or without RTV.

One final area of interest in this comparison is the steady state pressure reading after the shocks have passed. As figures 4-15 and 4-16 show, when RTV silicone is

added to the sensors, the result is a higher indicated steady state pressure. These plots also show the full view of a shock wave passing the two sensors twice. The first pair of spikes is the incident shock wave while the second pair is the reflected shock wave. The two plots represent two different runs which had nearly identical pressure differences prior to the bursting of the diaphragm.

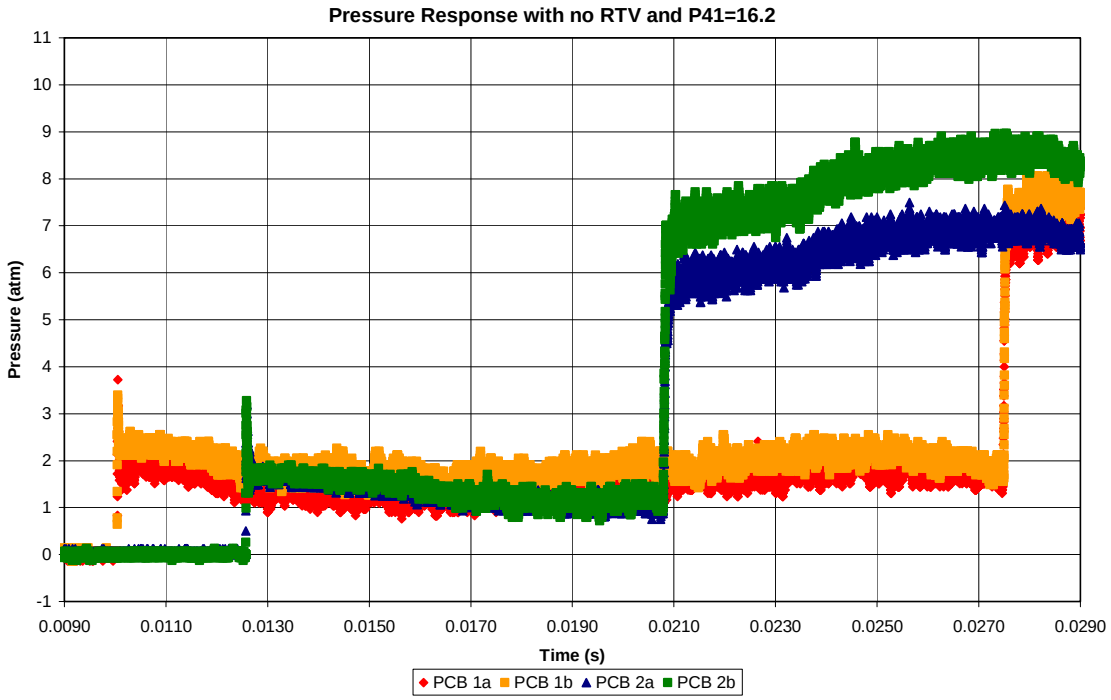

Figure 4-15: Pressure response of sensors with no RTV coating applied

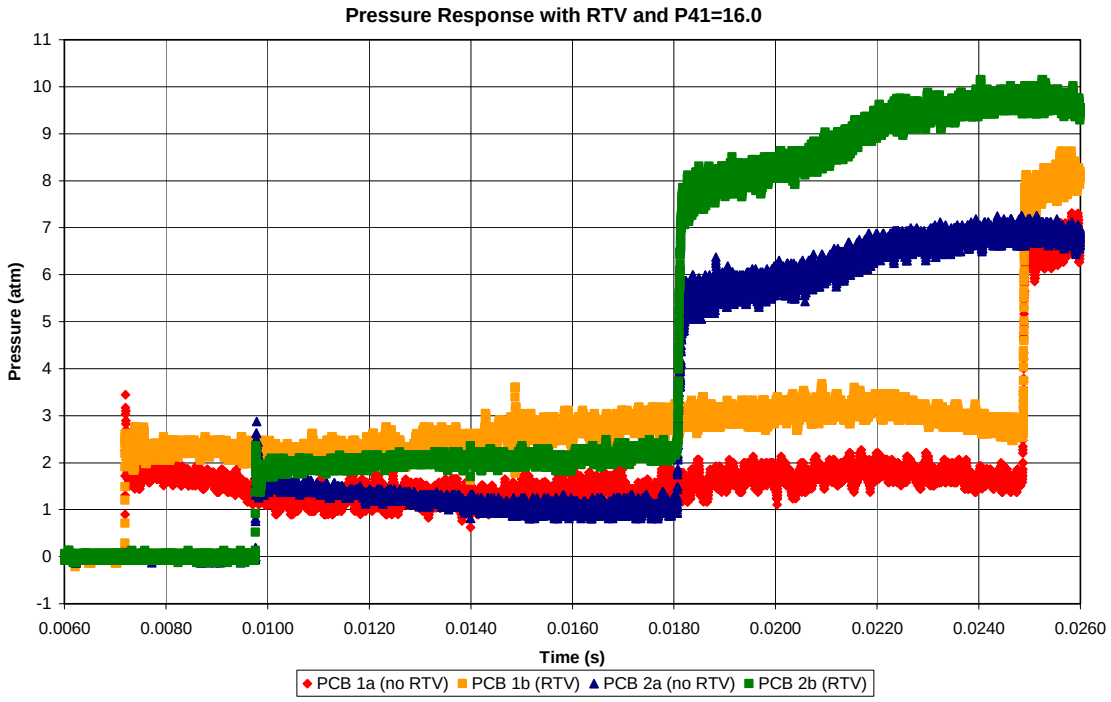

Figure 4-16: Pressure response of sensors with RTV coating on sensors 1b and 2b

The sensors with the coating of RTV silicone discharge to zero less quickly than those without the coating and show higher overall pressures. While the response to the spikes in pressure due to shock waves are the same as that of the sensors without the coating, the sensors with the coating respond with a higher steady state pressure that makes the difference between the two sensors nearly twice as great as it was when none of the sensors had the coating. This could be caused by the fact that when no coating has been applied to the sensors, they sensor itself is recessed in the casing. After RTV silicone has been applied, the effective surface of the sensor becomes flush with the sensor casing and is more exposed to the flow. The higher steady state pressure should be viewed as positive since it is unlikely that the sensors will indicate a pressure that is higher than the actual pressure in the tube. Therefore, it is safe to state that no negative impacts of the RTV silicone on pressure response were found in these tests. It is also

important to note that while plots for only four tests were shown in this section, results from every test were nearly identical with variations occurring based on shock speed and strength.

4.6 Ion Sensor Sensitivity

Experiments were conducted using helium as the driver gas and vacuumed air as the driven gas to develop a high Mach number in an attempt to ionize air and determine the threshold of the ion sensors for the detection of ions. The diaphragms used were two, 0.0126 mm thick stainless steel plates with etchings placed against each other in the same diaphragm station with the etching of each plate facing the driven side of the tube. Eleven tests were performed. However, investigation subsequent to the completion of 7 tests revealed that one of the *PCB* sensors being used to measure the wave speeds had become unseated from its housing and had been giving erroneous data since the second test. Therefore, all wave speeds for the tests after the second are inconclusive. This problem did not affect any prior tests with this sensor as two *PCB* sensors were located at the same station and had excellent agreement throughout the research. Five of the tests conducted provided consistent and reliable data with Mach numbers varying from 7.04 to 8.07.

The sensitivity of the ion sensors is determine by whether the sensors show a spike when the shock wave passes. The wave speed of each shock is measured by *PCB* pressure transducers. One pressure transducer and one ion probe were located at stations 1 and 2. A spike from the ion sensors would indicate that the shock wave caused the air to ionize and complete the circuit thereby discharging the sensor.

In only one of 11 runs did the ion sensor show a spike and in that case, the spike occurred only on the incident shock wave traveling at Mach 7.04. In all other tests including shock waves as fast as Mach 8.07, the ion sensors showed no response. Figure 4-17 shows the spikes of the ion sensors. The ion sensors are calibrated in arbitrary units but are shown here along with pressure transducers on a pressure scale in atmospheres.

Uncertainty is present in the experiment due to gas contamination. The tube cannot be fully evacuated before being filled with helium. Therefore, some air remained to mix with the helium which should slightly lower the shock wave although not by a noticeable amount. In addition, the tube was not flushed with air at the end of every run to clear all helium from the driven section. Helium left in the driven section should increase the wave speed while decreasing the Mach number and the temperature rise. If this did occur, it is not noticeable in the data as the wave speeds stayed below the speeds predicted by the analytical solution for helium driver and air driven sections.

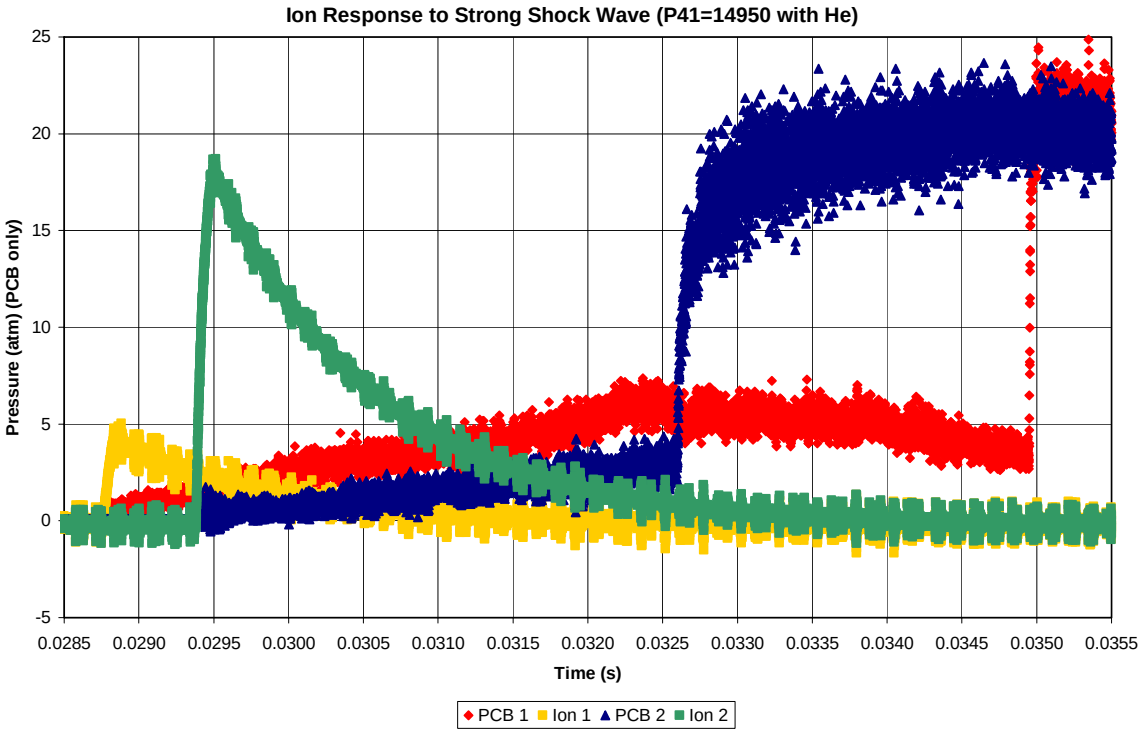

Figure 4-17: Pressure and ion response to Mach 7.04 shock wave (ion scale arbitrary)

The test that provided the ion response was the first tests conducted using the helium and the first test using these ion sensors. It is unclear what caused the ion sensors to spike on this shock wave but the ion spikes occurred at the exact time that the pressure transducers at the same respective locations registered a pressure spike from the passing wave. It is possible that impurities could have been present in the helium or that some cutting fluid or other flammable liquid could have remained on the ion sensors since they had not been used before. In the case of the sensors, had some flammable agent been left on the electrode, the ignition time would have had to been instantaneous to the passing of the shock wave on the order of 1 μs to show the spike as the shock passed and this ignition time is too fast to make this a plausible explanation. A final theory is that the bursting metal diaphragms could have released sparks in this case only that traversed the

tube with the incident shock wave but did not reflect. In any case, the results were not reproducible and cannot be conclusive in the cause.

Because 10 other tests showed no response from the ion sensors regardless of the speed of the wave, it can be stated that, for the range of conditions tested, the ion sensors are unable to detect the ions created by a hypersonic shock wave through air. When applied to the use of the sensors in the PDE, however, it can not be concluded that the sensors will not detect a shock wave through the air-fuel mixture in the tubes. Further research should be conducted on shock waves through air-fuel vapor mixtures to determine whether any additional ions are created by this event.

4.7 Wave Speed Progression

Because of unsteady flow from the bursting of the diaphragm as well as viscous effects, the speed of the shock wave varies throughout the shock tube. It is desirable to measure the speed of the wave as close to the peak location as possible in order to accurately assess the performance of the tube when compared to the analytical equations and the *CHEMKIN* results. Tests were conducted using 3 sensors at three stations in the tube. *PCB* pressure transducers were positioned at stations 1 and 2 while an *Endevco* transducer was used at station 3. The average speed of the wave was determined between each pair of sensors. Figure 4-18 shows the pressure response of a test conducted with 3 sensors using air in both sections and no RTV silicone on either of the *PCB* pressure transducers.

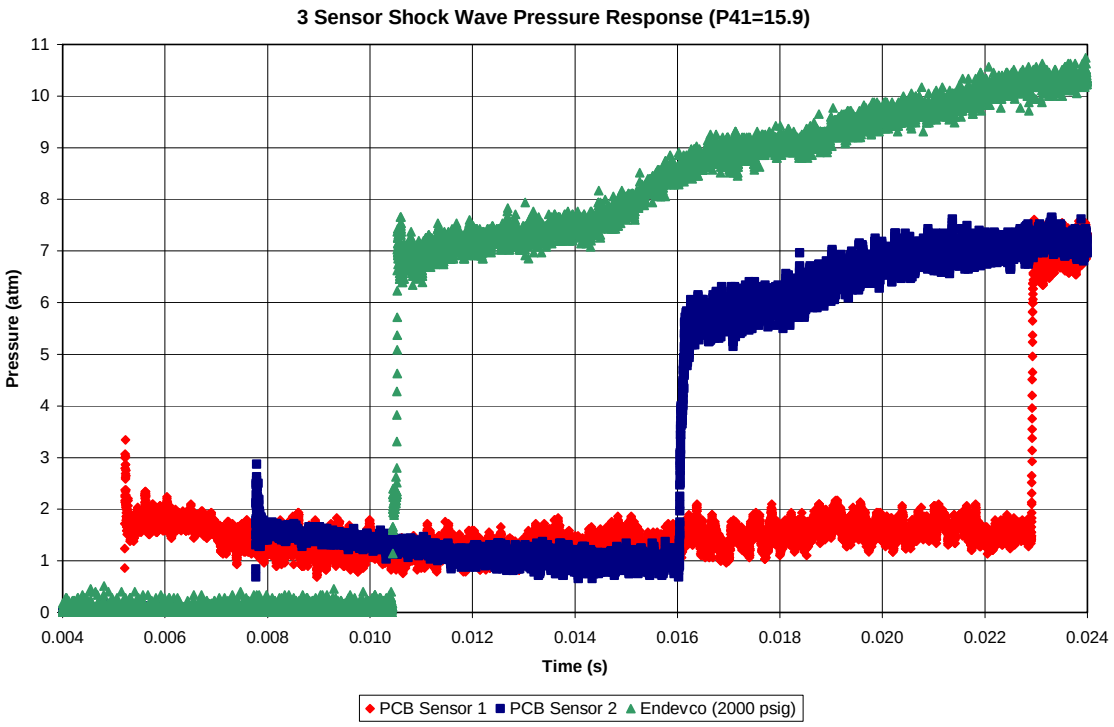

Figure 4-18: 3-sensor pressure response to shock wave

The spike of the *Endevco* sensor appears to be one large spike, but, because this sensor was located 1.5 cm from the closed end of the tube, it sensed both the reflected and the incident shock at almost the same time. In all tests, the shock wave velocity was greater between the first two sensors than it was between the second two. In addition, as the velocity of the shock wave increases, the drop in velocity from the first set to the second set increases. For the reflected wave, nearly every test showed a higher velocity between sensors 3 and 2 than between sensors 2 and 1 as the shock wave returned toward the center of the tube. This is likely due to viscous effects and unsteady flow in the shock tube. Mach numbers in these tests ranged from 1.69 to 3.58.

4.8 Shock Tube Performance

In order to evaluate the performance of the shock tube, it must be compared to the analytical, ideal gas solution as well as applicable results from CHEMKIN. The most obvious comparison comes from Figure 4-1 which shows expected Mach numbers generated by given pressure ratios. In all experiments conducted, the low speed waves under Mach 3 achieved an experimental Mach number within 7% of the theoretical Mach number from the analytical solution. As the velocity dropped, the experimental data became closer to the ideal prediction. When Mach numbers approached 4 with an air driver and 8 with a helium driver, the experimental Mach number remained within 9% of the theoretical Mach number. All experimental Mach numbers were below the theoretical predictions as expected. Figure 4-19 and 4-20 show the pressure ratio versus the incident shock Mach numbers. Figure 4-20 is the low speed portion of Figure 4-19.

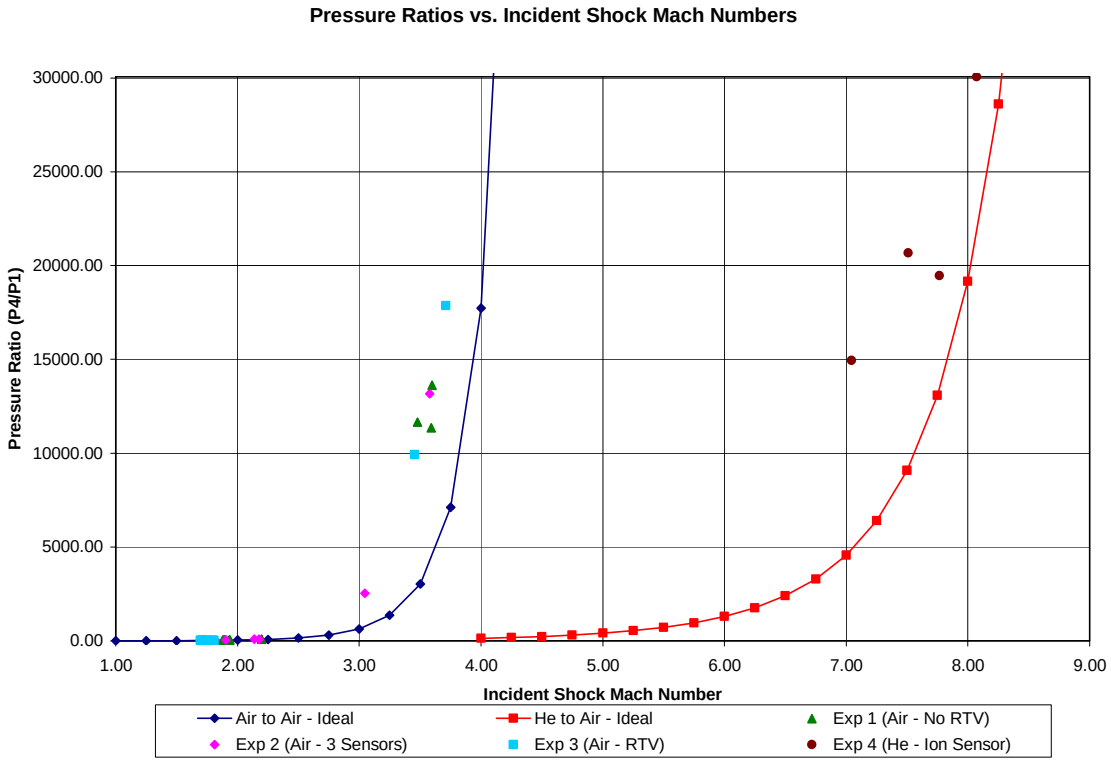

Figure 4-19: Pressure ratios versus experimental (points) and theoretical (curves) Mach numbers

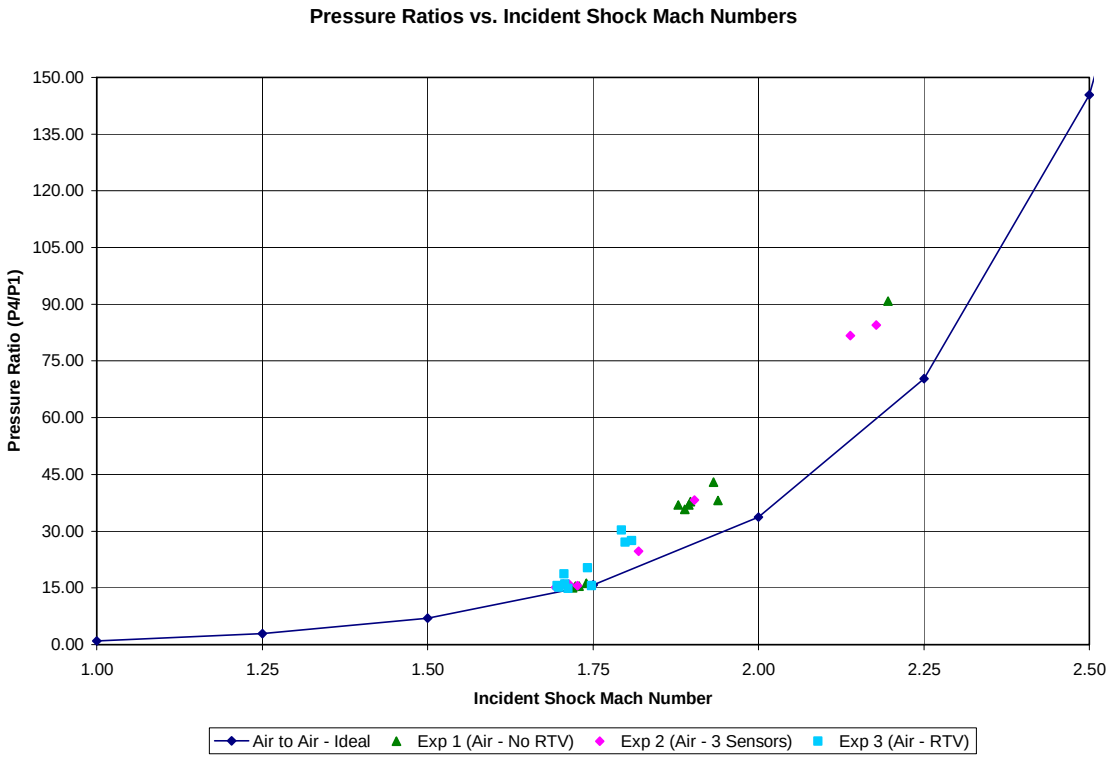

Figure 4-20: Pressure ratios versus experimental and theoretical Mach numbers (Low Speed)

The reflected shock wave velocity prediction was not as accurate as the incident Mach number prediction. For both the theoretical ideal case and the real gas case in CHEMKIN, the experimental data fell below the predicted values. In fact, rather than the reflected shock velocity rising as the incident shock velocity rises, in all tests using air as both the driver and the driven gas, as the incident shock velocity rose, the reflected shock velocity fell slightly. With incident shock velocities nearing 1300 m/s, the experimental reflected shock velocity was only 47% of the CHEMKIN predicted value and only 40% of the theoretical value from the ideal gas equations. At the higher velocities with the helium driver, the reflected shock prediction faired slightly better with 25% error when compared to CHEMKIN and 42% error when compared with the ideal gas prediction. This severe attenuation is likely caused by viscous effects and heat transfer as well as

sensors protruding into the tube and empty ports providing cavities. Figure 4-21 shows the CHEMKIN and ideal gas predictions as well as the data points from all test runs.

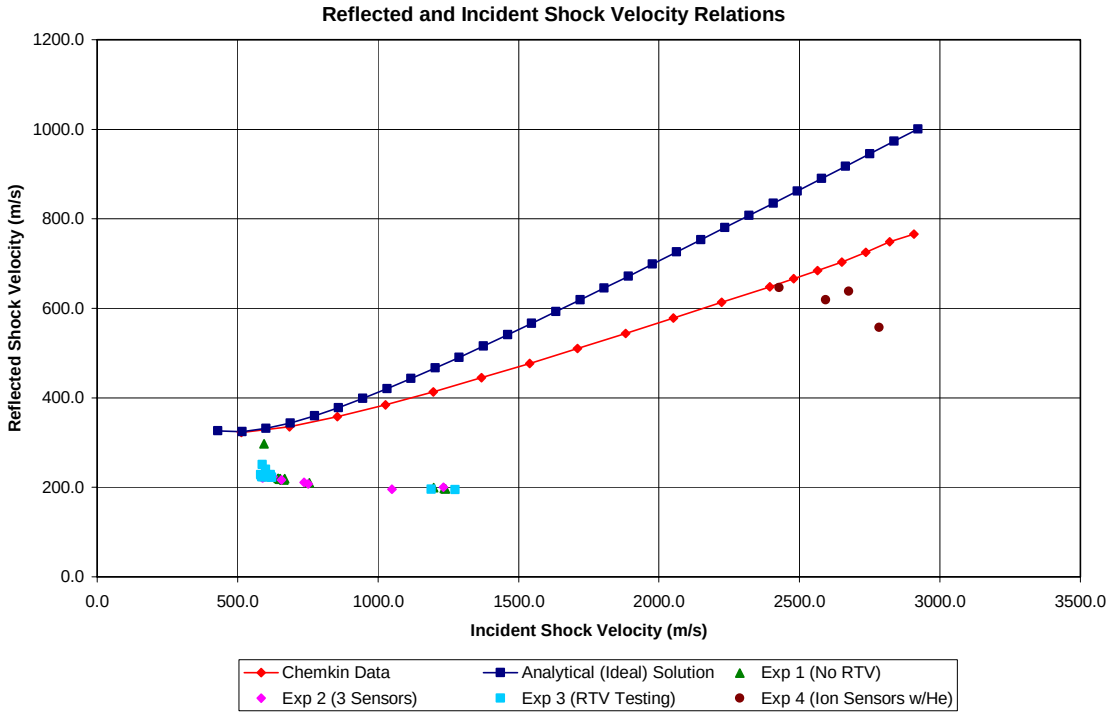

Figure 4-21: Experimental reflected shock velocities compared to predicted velocities

4.9 Experimental Challenges

As previously discussed, the diaphragms used in this research were extremely inconsistent and the burst pressure of each diaphragm was nearly impossibly to predict thereby making it difficult to design a test to achieve certain Mach numbers. In addition, diaphragms occasionally did not fully petal and open up when the burst occurred. Instead, only one axis of the etching would separate or only two of the four petals would fold out of the way of the flow. The single axis burst created significant problems as the data was not useable. Rather than two large pressure spikes (incident and reflected shocks) followed by a gradual fall to a steady state pressure when only one axis opened, a

series of ten or more slow and weak shocks slowly jumped the pressure to the steady state pressure. While spikes are visible and sensor comparison is possible, the variation from the predicted Mach number based on the pre-burst pressure ratio climbed to nearly 40% error vice the less than 10% error that was observed on full breaks.

It is also fair to say that for a tube that is vacuumed, the pressure transducers used in this research had too large a range for accurate measurement. The pressure rise from each shock wave is determined by a pressure ratio based on the speed of the wave. Because the initial pressure of the driven section was so low (0.004 atm) after the vacuum was used, the pressure spike of the incident shock wave was barely detected by the pressure transducers. In this case, it would have been ideal to have transducers which are sensitive to lower pressures rather than having transducer that can detect pressures greater than 150 atm. However, this is a limitation of the shock tube. The steady state pressure in the tube after all shocks have stopped is higher than 50 atm in some cases with spikes taking pressures even higher. Pressures of this magnitude cannot be placed on sensors which are designed for lower pressures without damaging them. It is necessary to vacuum the driven section of the tube in order to achieve high Mach numbers regardless of which gases are used. As a result, the less sensitive sensors must be used.

4.10 Chapter Summary

Sensor experiments on the AFIT 2-inch shock tube utilized various pressure ratios to achieve various Mach numbers in an effort to characterize the performance of both the shock tube and the sensors. Pressure transducers coated with a layer of RTV silicone

showed no degradation in the accuracy of the measurements when compared to sensors without the silicone. In some cases, the sensors became more sensitive due to the RTV silicone coating and showed a higher steady state pressure. The ion sensors tested were unable to consistently detect any ions in the shocked air. The single instance of detection is insufficient evidence to conclude that the spike was caused by ions created by the shock wave alone.

The shock tube itself performed in an acceptable manner relative to the equations predicting the speed of each shock. The Mach numbers achieved were within 7% of the expected Mach number at speeds below Mach 3 and with 9% and higher Mach numbers. However, the reflected shock velocity achieved did not conform to expectations. The experimental velocities held as much as 60% error when compared to the ideal shock tube equations and as much as 53% error when compared to results from CHEMKIN which simulates real gas effects in the tube.

5 Conclusions and Recommendations

5.1 Conclusions

The AFIT 2-inch shock tube is fully functioning as an experimental apparatus for engineering research. Sensors ports have been installed and data acquisition equipment has been configured for efficient use in measuring wave speeds and pressure changes in the tube. The shock tube is capable of producing shock waves near Mach 4 with air on both sides of the tube and shock waves in excess of Mach 8 when using helium as the driver gas. Mach numbers achieved consistently fell within 7% of the theoretical prediction at wave speeds below Mach 3 and within 9% at wave speeds above Mach 3. However, the current setup does not provide for an efficient reflection of the incident shock wave as errors are as high as 53% when compared to CHEMKIN real gas predictions. In experiments with three sensors, the results showed that the peak velocity of each shock wave is achieved within 3 meters of the diaphragm.

In the sensor tests comparing RTV silicone coated transducers with uncoated transducers, the experimental results show that the RTV silicone coating used to insulate the *PCB* piezoelectric dynamic pressure transducers has no negative effect on the sensitivity or the speed of response of the sensors. In the tests conducted, the sensors coated with the RTV silicone reached higher steady state pressures than were reached when no coating had been applied indicating that the coating may actually improve the response of the sensors.

The ion sensor probes fashioned from sparkplugs were unable to consistently detect ions created by shock waves between Mach 7 and Mach 8.2. It is therefore

impossible to determine the threshold for detection of the sensors. A response to the shock was seen in only the first test conducted and was not reproducible through 10 further tests. It must, therefore, be assumed that the single reading was the result of circumstances other than the hypersonic shock wave through air as the wave which caused the reading was one of the slower waves produced in the testing. Consequently, it can be concluded that the ion sensors are unable to detect the ions created by a Mach 8 shock wave propagating through air.

5.2 Recommendations

While the AFIT 2-inch shock tube has been reassembled and prepared for further experimental research, there are several areas which could be improved upon to ensure that future research is more accurate and efficient. The inconsistencies in the diaphragms, whether due to age or machining errors, must be resolved. New diaphragms must be manufactured with precision etching or no etching at all to create a more consistent burst pattern. Coupling two diaphragms together to achieve a higher burst pressure is extremely inconsistent and must be replaced by thicker diaphragms or shallow etching. A more reliable and repeatable method is to build a mechanical bursting mechanism, such as a punch, that can be installed in the shock tube and remotely operated to rupture the diaphragms. This would also solve inconsistencies with burst pressures but would be most effective if coupled with new diaphragms.

While the results have shown that the peak shock wave velocity occurs within 3 meters of the diaphragm, because of the mixing of the gases, the most accurate results can be achieved by placing the sensors as close to the end of the tube as possible. In the

current setup, gas mixing was allowed to occur at the locations of each sensor before the reflected shock arrived making chemical reactions less predictable. This is not as critical in tests where air is used on each side of the diaphragm but becomes important when gases other than air are used.

The sensor ports on the shock tube connecting plates were machined in an inaccurate manner that caused offsets in the sensor locations and allowed the sensors to protrude into the tube. Special care should be taken in getting the remaining connecting plates machined for the installation of sensors in a matter that produces more accurate and consistent results without such large correction factors. Ports may also be machined on the tube itself which would allow sensors to be located at much closer intervals.

The data for the pressures on the driver and driven sides of the tube were taken manually by recording voltages from a multimeter. The multimeter gives average voltages and is constantly changing so the peak voltage recorded will only provide an estimated peak pressure. These sensors should be linked into a low-speed data acquisition system or can be used with the high-speed Online Wave Speed if ports are available. Online Wave Speed can accept 16 channels but more data acquisition cards are needed in the computer itself as the current card is limited to 4 channels.

Several of the pneumatically operated high pressure valves which control in gas flow into and out of the tube have deteriorated to the point that they now possess significant leaks. These valves must either be replaced or reseated to ensure proper seals and safe and effective operation of the shock tube.

Finally, when using gases other than air inside the tube, extreme diligence must be used to ensure that all gas in the tube has been flushed in between tests.

Contamination in the driven section can be much more detrimental to the experimental data than contamination in the driver.

Appendix A.

Equipment List

RTV Silicone - *VersaChem* High-Temp Red Silicone Type 650. 5000 psi pressure limit. 200 K to 615 K temperature range (sustained temperatures).

Vacuum Transducer – *Endevco* 15 psia. Model 8350C-15. S/N 11382.

Driven Transducer – *Endevco* 2000 psig. Model 8510B-2080. S/N 10445

Driver Transducer – *Viatran* 2000 psig. Model 104. S/N 150160.

Driver Transducer Reader – *Agilent* 6.5 Digit Multimeter. Model 34401A. S/N SG41015990.

Ion Sensor – *NGK* 7499 C9E Kawasaki Motorcycle Spark Plug. 10 mm thread reduced to 3/8" 24.

Pressure Transducers – *PCB Piezotronics* ICP Dynamic Pressure Transducers.

Model #	Serial #	Amplifier Model #	Amplifier Serial #	Condition	Calibration (psi/V)	Station	RTV?
102M232	15010	PCB402M10	8402	Good	1037	5ft / F / 1	No
102M232	15008	PCB402M10	8401	Good	1064	5ft / R / 2	Yes
102M232	18000	PCB402M10	8704	Good	940	10ft/ F / 3	No
102M232	17993	PCB402M10	8578	Good	985	10ft/ R / 4	Yes

Signal Conditioner – *PCB Piezotronics* ICP Sensor Signal Conditioner Model 482 Series.

Thermocouples – *Omega* type-K. 1/8 inch diameter and 1/16 inch diameter.

Thermocouple Display – *Omega* TrueRMS Supermeter. Model HHM290. S/N 0000356.

Data Acquisition Board – *National Instruments* PCI-6110.

Data Input Box – *National Instruments* BNC-2120.

Appendix B.

AFIT 2-inch Shock Tube
Operating and Safety Procedures

The checklists detailed below outline the standard operating procedures for safe and efficient operation of the AFIT 2-inch Shock Tube. Failure to comply with these procedures could result in serious injury and severe damage to equipment. Where valve names are indicated, valves labeled with a "P" can be operated from the instrument panel while valves labeled with an "M" must be operated manually.

Checklist for Opening Shock Tube

1. Turn on the control panel and check to see that all valves are in the following positions:

P-1 Closed	P-5 Open	M-2 Closed	M-8 Open
P-2 Closed	P-6 Open	M-4 Open	M-9 Closed
P-3 Open	P-8 Open	M-5 Closed	
P-4 Open	P-9 Open	M-6 Open	

2. Open manual 90 degree valve for 100 psi shop air. After observing no water exiting valve P-3, close valve P-3.

3. Check to see that the pneumatic ram for opening and closing the tube is unplugged and manual valve out of regulator for high pressure air is closed.

4. Use large wrench to loosen large fitting. If necessary, use smaller wrench to loosen large fitting until it can be turned by hand. Unscrew large fitting until smaller inner threads are visible.

5. Check to see that the supports of the driver section are clear of any debris as the entire section will move away from the driven side by about one foot.

6. Plug in the pneumatic ram. Ensure that all persons are clear of the driver section. Push the switch next to the ram in short pulses to move the driver away from the driven section. Check to see that the driver is a sufficient distance from the driven end so that the diaphragm casing can be removed. CAUTION: UNPLUG THE PNEUMATIC RAM PRIOR TO REMOVING THE DIAPHRAGM CASING.

7. With the ram unplugged, remove the diaphragm casing. If the casing has remained inside the driver section, pull the diaphragm out by the slots using the hooks.

Checklist for Installing New Diaphragms

1. Follow the checklist to open the shock tube.

2. Observe the alignment of the sections of the casing in order to properly reassemble them. Unscrew the two bolts in the end of the diaphragm casing. Remove the upper portion of the casing to expose the housing for the first diaphragm. NOTE: *The first diaphragm is the diaphragm in direct contact with the gas in the driver and will explode toward the second diaphragm*.

3. If two diaphragms will be used, remove the middle section of the casing as well to expose the housing for the second diaphragm.

4. Install the diaphragms with the holes aligned with the holes in the casing. If the diaphragm is etched on one side, install the etched side facing downward or toward the driven section.

5. Reassemble the casing and ensure that the bolts are tight. The diaphragms may move once installed even with tight bolts. This movement will be restricted once the diaphragms are exposed to high pressures.

Checklist for Closing Shock Tube

1. Check to see that the pneumatic ram for opening and closing the tube is unplugged and manual valve out of regulator for high pressure air is closed.

2. Check to see that the rubber gaskets on each end of the diaphragm casing are present. Install the diaphragm casing in the driver side by sliding it into the tube with the bolt side going in first. Make sure that the slotted side is visible with the slots on opposite sides of the casing aligned horizontally. When fully installed, the end of the casing should be nearly flush with the end of the open driver side.

3. Plug in the ram and toggle the switch to the close position in pulses to avoid slamming the two sides together. While this may be unavoidable, it is best not to do it in excess. Once the two sides meet, check the alignment and apply force to the driver side as necessary to align the tubes.

4. Manually tighten the large fastener until it is hand tight. Toggle the ram switch to close and hold for 3 seconds.

5. Repeat step 4 until the large fastener can no longer be manually tightened. Unplug the pneumatic ram. Use the large wrench to tighten the large fastener with as much force as possible until no motion is observed.

Checklist for Operating the Shock Tube Without a Vacuum

1. Plug in the shock tube control panel and make sure valve P-3 is open. Ensure that the shock tube is closed properly with a diaphragm installed. Turn on the 100 lb shop air. Close valve P-3 as long as no water can be heard in the 100 lb air. TURN ON 'TEST IN PROGRESS' LIGHTS ON BOTH DOORS OF THE LAB.

2. Set all valves to the following positions:

P-1 Closed	P-5 Closed	M-2 Closed	M-8 Open
P-2 Closed	P-6 Open	M-4 Open	M-9 Closed
P-3 Closed	P-8 Open	M-5 Closed	
P-4 Open	P-9 Closed	M-6 Open	

3. Check to see that the master pressure switch (on control room wall) is set to the closed position. Set the regulator pressure at the desired maximum pressure for the tube. If the pressure rises above the desired maximum pressure, open the regulator release valve to the left of the regulator. Check the regulator pressure after it becomes steady. If it is still too high, turn the regulator dial a few turns counter-clockwise and open the valve again. Repeat until the regulator pressure is as desired. Open the manual 90 degree valve for the high pressure air out of the regulator.

4. Move all personnel in the lab into the control room and shut the door.

5. If using only a single diaphragm in the upstream location, skip to step 8.

6. Open the master pressure valve on the control room wall and allow the entire tube to pressurize to 80% of the downstream diaphragm's burst pressure. At 80% of burst pressure, close the master pressure valve. Close valve P-4. Open the master pressure valve and fill the driver section to 80% of the upstream diaphragm's burst pressure. Close the master pressure valve.

7. When ready to commence testing, open valve P-5 to vent the region between the two diaphragms to atmospheric pressure. When the pressure difference between the two sides is sufficient, the diaphragms will burst. Skip to step 9.

8. Close valve P-4. When ready to commence testing, open the master pressure valve and allow the tube to pressurize until the diaphragm bursts.

9. Immediately after the diaphragm(s) bursts (or if the diaphragm(s) does not burst after pressures are constant), close the master pressure valve, lock the doors using the solenoid switch, and open valve P-9 and valve P-4. This will vent the entire tube to atmospheric pressure.

10. Close the 90 degree manual valve from the regulator and turn the regulator pressure dial to zero. Use the regulator vent to release any pressure.

11. If the diaphragm burst, use the checklist for opening the shock tube. If the diaphragm held, repeat the operating procedures using a higher regulator pressure or use the checklist for opening the tube and installing a new diaphragm.

12. When operations on the shock tube are complete, open valves P-9 and P-5. TURN OFF 'TEST IN PROGRESS' LIGHTS ON BOTH DOORS OF THE LAB. Open valve P-3 for the 100 psi shop air to vent. Close the 90 degree manual valve for the shop air. Turn off the control panel.

Checklist for Operating the Shock Tube With a Vacuum

1. Turn on the first stage of the vacuum pump (left box). After at least 4 minutes, turn on the second stage by selecting manual with the switch on the right box. Plug in the shock tube control panel and make sure valve P-3 is open. Ensure that the shock tube is closed properly with a diaphragm installed. Turn on the 100 lb shop air. Close valve P-3 as long as no water can be heard in the 100 lb air. TURN ON 'TEST IN PROGRESS' LIGHTS ON BOTH DOORS OF THE LAB.

2. Check to see that the master pressure switch (on control room wall) is set to the closed position, and set all valves to the following positions:

P-1 Closed	P-5 Closed	M-2 Open	M-8 Open
P-2 Open	P-6 Open	M-4 Open	M-9 Closed
P-3 Closed	P-8 Open	M-5 Closed	
P-4 Open	P-9 Closed	M-6 Open	

3. To begin vacuuming the tube, open the 90 degree main vacuum valve. The tube may take as long as 30 minutes to vacuum to the lowest possible pressure. (Note: Under the current configuration, the entire tube can only be vacuumed if a single diaphragm is used in the upstream station. A diaphragm in the downstream station will prevent communication between the driven section and the driver section. In either case, the driven section can always be vacuumed.)

4. Set the regulator pressure at the desired maximum pressure for the driver section. If the regulator pressure rises above the desired maximum pressure, open the regulator release valve to the left of the regulator. Check the regulator pressure after it becomes steady. If it is still too high, turn the regulator dial a few turns counter-clockwise and open the valve again. Repeat until the regulator pressure is as desired. Open the manual 90 degree valve for the high pressure air out of the regulator.

5. When the vacuum has reached the desired pressure, close valve M-2 and P-2. Move all personnel in the lab into the control room and shut the door.

6. If using a single diaphragm setup, skip to step 8. If using a double diaphragm configuration (only the driven section has been vacuumed), open the master pressure valve on the control room wall and allow the entire tube to pressurize to 80% of the downstream diaphragm's burst pressure. At 80% of burst pressure, close the master pressure valve. Close valve P-4. Open the master pressure valve and fill the driver section to 80% of the upstream diaphragm's burst pressure. Close the master pressure valve.

7. When ready to commence testing, open valve P-5 to vent the region between the two diaphragms to atmospheric pressure. When the pressure difference between the two sides is sufficient, the diaphragms will burst. Skip to step 9.

8. Close valve P-4. When ready to commence testing, open the master pressure valve and allow the tube to pressurize until the diaphragm bursts.

9. Immediately after the diaphragm(s) bursts (or if the diaphragm(s) does not burst after pressures are constant), close the master pressure valve, lock the doors using the solenoid switch, and open valve P-9, P-1, and P-4. This will vent the entire tube to atmospheric pressure.

10. Close the 90 degree manual valve from the regulator and turn the regulator pressure dial to zero. Use the regulator vent to release any pressure.

11. If the diaphragm burst, use the checklist for opening the shock tube. If the diaphragm held, repeat the operating procedures using a higher regulator pressure or use the checklist for opening the tube and installing a new diaphragm.

12. When operations on the shock tube are complete, open valves P-9 and P-5. TURN OFF 'TEST IN PROGRESS' LIGHTS ON BOTH DOORS OF THE LAB. Open valve P-3 for the 100 psi shop air to vent. Close the 90 degree manual valve for the shop air. Turn off the control panel.

Special Instructions for using driver gases other than air

When using a gas other than air in the driver side, follow the procedures for operating the shock tube with a vacuum. In this case, a single diaphragm must be used to ensure that the driver side can be vacuumed. This gas can be tapped into the tube through the same piping as the air and can use the same regulator as the air provided that the high pressure air is turned off. In this manner, the same procedures can be used. Do not forget to close valve P-4 prior to releasing the high pressure gas into the tube. In addition, high pressure air should be used in between runs to flush the driven section of the tube to remove the gas being used as the driver.

Driver/ Double Diaphragm

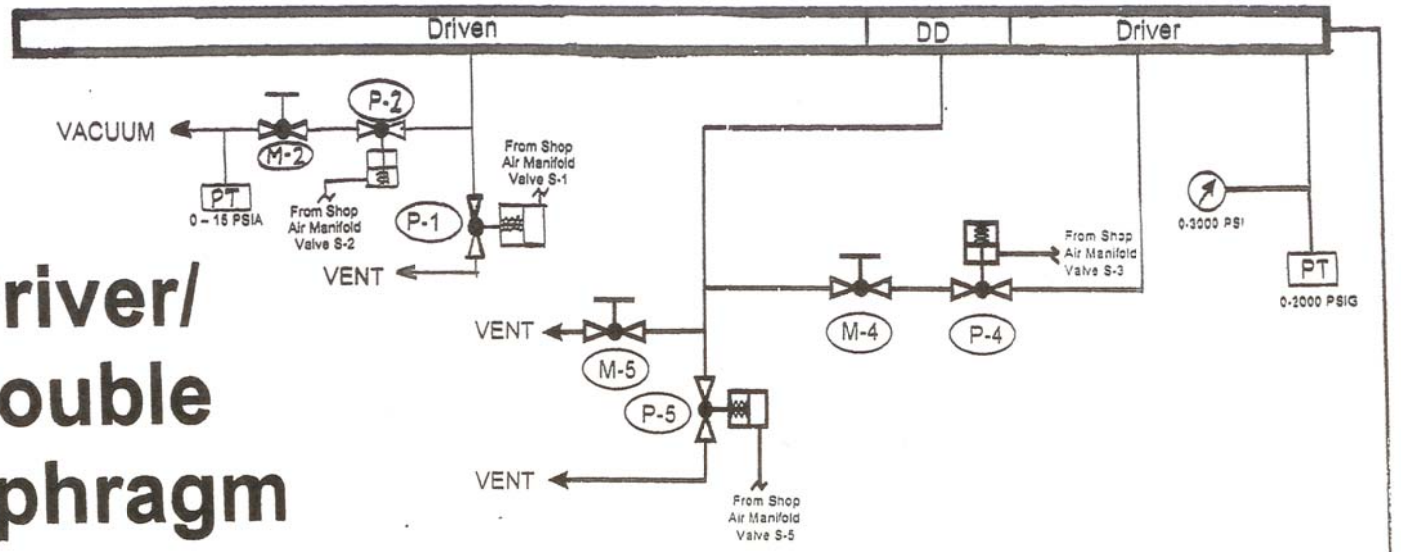

AFIT 2-Inch Shock Tube

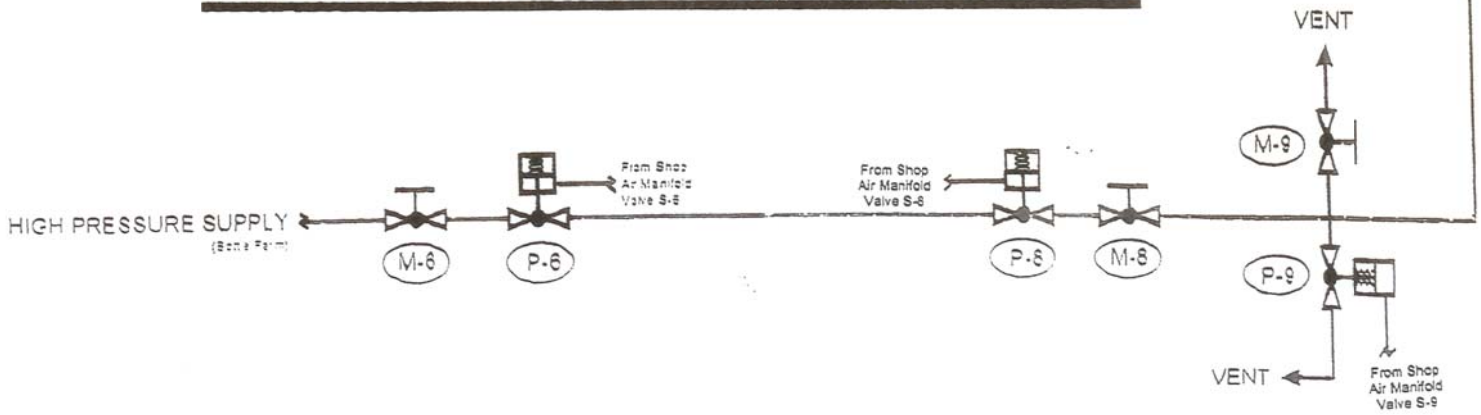

Appendix C.

Procedure for Operation of Data Acquisition System

1. Turn on Signal Conditioner and verify that all 4 channels are in the green. Open Online Wave Speed.

2. Scroll left and check the voltage range under 'Master' to ensure each sensor has the applicable voltages for the experiment. Scroll back to center.

3. Check to see that the green button in the upper left reads 'continuous buffer'. Set the 'Scan Rate' (scans per second) to 2.00E+6. Set the 'Scans to read from buffer' to 2.00E+6. This will take one second of data. Set the 'Scans to read at a time' to 1.00E+4. Set the 'Threshold' in Volts to a value which the data will reach only when the shock has occurred. The default value is 0.050 V.

4. Click on the 'Transducer' button. Check that all transducers are listed with the correct serial numbers and calibrations. Make sure the transducers being used are selected on the right column in the order in which the data is imported. Click 'Done'. Click 'Tube Setup'. Set the transducer locations in the tube. Click 'Done'.

5. Check to see that the green light next to the 'start' button at the top is lit. If it is not, click the 'Done' button under 'Analyze' (should be next to the green light) to send the green light to the top.

6. After the switch is turned on to begin pressurizing the tube, click the 'Done' button at the top of the screen to begin scanning for data. When the data spikes above the threshold, the one second block in which the spike occurred will be dumped to the window in the middle of the screen.

7. Adjust the width in the 'Window Control' box to change the number of windows and adjust the offset to center the desired data in the middle of the screen. When the desired data is in the screen, uncheck the 'Write all data' box in the 'Data Archive' window. Then click 'Save' to save the data. When the green light next to the 'Save' button goes out, the data is saved. The program creates a folder named with the current date on the D:/ drive. The files are named by run number. The name and number may be changed in the box but the number will change automatically with each run. Data may be further analyzed using PT Reader.

8. When finished analyzing the data on the screen, click the 'Done' button under 'Analyze' and the light will go on next to the start button and another test can be completed. To run more tests, repeat steps 6 and 7.

Procedure for Analyzing Data with PT6

1. Open PT reader and select the file to analyze.

2. Adjust the scan window so that it is equal to "scans remaining".

3. Click "Max View" until the view size is equal to the scan window. Click "Read".

4. Adjust "skip scans" for the offset to the right. Adjust the view size to bring the desired data into the screen with extraneous data eliminated. (Note: to save the file in *Excel*, the "view size" divided by the "skip points" plus one must be less than or equal to 30,000. Skipping points will reduce the effective scan rate.)

5. Click "Generate."

6. When the file has been generated in the lower window, either analyze the data or click "Write" to save the data. Save the file in the following format: name.xls. This file is not an *Excel* file but can be opened in *Excel* and converted to that file type.

Checklist for Tests without use of the Vacuum

1. Close the shock tube.

2. Set the regulator to the desired driver pressure for the test. Open the manual 90˚ regulator valve.

3. Turn on the thermocouple display.

4. Check valve status as follows:

P-1 Closed	P-5 Closed	P-9 Closed
P-2 Closed	P-6 Open	P-10 Closed
P-3 Closed	P-7 Closed	
P-4 Closed	P-8 Open	

5. Record ambient temperature and pressure.

6. Turn on high pressure air with main regulator valve and turn on the data acquisition system immediately after air begins to flow.

7. Observe the pressure reading for the driver section until the diaphragm bursts and immediately record the value along with the driver and driven temperatures at the time of the break.

8. Quickly shut off the pressure to the tube with the main regulator valve, and open valves P-5 and P-9 to vent the entire tube. Ensure that the door to the control room is closed as the venting air is very loud.

9. Save the data recorded by Online Wave Speed.

10. Turn off the thermocouple display and close the manual 90˚ regulator valve.

11. Open the tube and change the diaphragm. (Return to item 1.)

Checklist for Tests with use of the Vacuum

1. Close the shock tube.

2. Open valve M-2 for the vacuum. Close valves P-5 and P-9 and open valve P-2. If using driver gases other than air, open valve P-4 as well.

3. After the tube has vacuumed to the desired pressure, close valves P-4 and P-2. Also close valve M-2. Record the pressure of the driven section. If the tube has no leaks, this pressure will hold until the diaphragm breaks.

4. Set the regulator to the desired driver pressure for the test. Open the manual 90˚ regulator valve.

5. Turn on the thermocouple display.

6. Check valve status as follows:

P-1 Closed	P-5 Closed	P-9 Closed
P-2 Closed	P-6 Open	P-10 Closed
P-3 Closed	P-7 Closed	
P-4 Closed	P-8 Open	

7. Record ambient temperature and pressure.

8. Turn on high pressure air with main regulator valve and turn on the data acquisition system immediately after air begins to flow.

9. Observe the pressure reading for the driver section until the diaphragm bursts and immediately record the value along with the driver and driven temperatures at the time of the break.

10. Quickly shut off the pressure to the tube with the main regulator valve, and open valves P-5 and P-9 to vent the entire tube. Ensure that the door to the control room is closed as the venting air is very loud.

11. Save the data recorded by Online Wave Speed.

12. Turn off the thermocouple display and close the manual 90˚ regulator valve.

13. Open the tube and change the diaphragm. (Return to item 1.)

Bibliography

Anderson, John D. Jr. *Hypersonics and High Temperature Gas Dynamics*. Reston VA: AIAA, 1989.

-----. *Modern Compressible Flow With Historical Perspective* (3rd Edition). New York: McGraw-Hill, 2003.

Bureau of Naval Weapons. *Handbook of Supersonic Aerodynamics, Section 18, Shock Tubes*. NAVORD Report 1488, Vol. 6. Washington: Government Printing Office, 1959.

Farnell, Lawrence C. *Iodine Dissociation in a Shock Tube*. MS thesis, AFIT/GAE/AA/80D-5. School of Engineering, Air Force Institute of Technology (AU), Wright-Patterson AFB OH, December, 1980 (ADA094760).

Gaydon, A.G. *Dissociation Energies*. New York: John Wiley & Sons Inc., 1947.

Gaydon, A.G. and I.R. Hurle. *The Shock Tube in High-Temperature Chemical Physics*. New York: Reinhold Publishing Corp., 1963.

Glass, I.I. *Shock Tubes: Part I*. Toronto: University of Toronto, 1958.

Hall, J. Gordon. *Shock Tubes: Part II*. Toronto: University of Toronto, 1958.

Hoffmann, Kaus A. and Steve T. Chiang. *Computational Fluid Dynamics: Volume II* (4th Edition). Wichita KS: Engineering Education System, 2000.

Kuo, Kenneth K. *Principles of Combustion*. New York: John Wiley & Sons, Inc., 1986.

Laderman, A.J., G.J. Hecht, R.A. Stern, and A.K. Oppenheim. "Flame Ionization During the Development of Detonation," *Proceedings of the 8th International Symposium on Combustion*. 199-206. 1960.

Martin, W.C. and others. "Ground Levels and Ionization Energies for the Neutral Atoms." National Institute of Standards and Technology, Physics Laboratory. n. pag. http://physics.nist.gov/PhysRefData/IonEnergy/ionEnergy.html. September 2003.

National Instruments PCI-6110/6111 User Manual. http://www.ni.com/pdf/manuals/370980a.pdf. May 2004.

PCB Piezotronics. "Introduction to Piezoelectric Pressure Sensors." http://www.pcb.com/tech_pres.html. March 2003.

Panzenhagen, Kristin L. *Detonation Branching in a PDE with Liquid Hydrocarbon Fuel*. MS thesis, AFIT/GAE/ENY/04-M13. Graduate School of Engineering and Management, Air Force Institute of Technology (AU), Wright-Patterson AFB OH, March, 2004.

Schneider, K.P. and Grönig, H. "Ionization Measurement in Shock Heated Argon with Microwaves and a Pulsed Langmuir Probe," *Proceedings of the Eighth International Shock Tube Symposium*. 44. London: Chapman and Hall, 1971.

Terao, K. and Yamamoto, K. "A Study on Ionization of Gases Behind Reflected Shock Waves by Double Probe Method," *Proceedings of the Eighth International Shock Tube Symposium*. 43. London: Chapman and Hall, 1971.

Tucker, K., P. King, and F. Schauer. "Detonation Wave Speed Measurements with Ion Sensors," 28th Dayton-Cincinnati Aerospace Science Symposium, Dayton OH, March 2003.

Vincenti, W.G. and C.H. Kruger, Jr. *Introduction to Physical Gas Dynamics*. Malabar FL: Krieger Publishing Company, 1986.

Vlcek, Kevin M. *An Investigation of the AFIT 2-inch Shock Tube as a Flow Source for Supersonic Testing*. MS thesis, AFIT/GA/ENY/94D-1. School of Engineering, Air Force Institute of Technology (AU), Wright-Patterson AFB OH, December, 1994 (AAL4890).

Wright, J.K. *Shock Tubes*. New York: Methuen's Monographs on Physical Subjects, 1961.

Zdenek, Jeffery S. *Ion Based Pressure Sensor for Pulse Detonation Engines*. MS thesis, AFIT/GAE/ENY/04-M17. Graduate School of Engineering and Management, Air Force Institute of Technology (AU), Wright-Patterson AFB OH, March, 2004.

Zdenek, Jeffery S. and Ralph A. Anthenien. "Ion Based High-Temperature Pressure Sensor." AIAA-2004-0470.

Vita

Ensign Robert J. McMillan graduated from Floyd E. Kellam High School in Virginia Beach, Virginia in June 1999. He attended the United States Naval Academy in Annapolis, Maryland where he graduated with distinction with a Bachelor of Science degree in Mechanical Engineering in May 2003. He was commissioned into the United States Naval Reserve (active status) upon graduation.

After graduation in June 2003, Ensign McMillan was assigned to the Immediate Graduate Education Program at the Air Force Institute of Technology Graduate School of Engineering and Management as part of a partnership with the Naval Postgraduate School. Upon graduation, he will begin training to become a Naval Aviator in Pensacola, Florida.

REPORT DOCUMENTATION PAGE

Form Approved
OMB No. 074-0188

1. REPORT DATE *(DD-MM-YYYY)*	2. REPORT TYPE	3. DATES COVERED *(From – To)*
04-06-2004	**Master's Thesis**	Jun 03 – Jun 04

4. TITLE AND SUBTITLE

SHOCK TUBE INVESTIGATION OF PRESSURE AND ION SENSORS USED IN PULSE DETONATION ENGINE RESEARCH

5a. CONTRACT NUMBER

5b. GRANT NUMBER

5c. PROGRAM ELEMENT NUMBER

6. AUTHOR(S)

McMillan, Robert J., Ensign, USNR

5d. PROJECT NUMBER

5e. TASK NUMBER

5f. WORK UNIT NUMBER

7. PERFORMING ORGANIZATION NAMES(S) AND ADDRESS(S)

Air Force Institute of Technology
Graduate School of Engineering and Management (AFIT/ENY)
2950 Hobson Way
WPAFB OH 45433-7765

8. PERFORMING ORGANIZATION REPORT NUMBER

AFIT/GAE/ENY/04-J07

9. SPONSORING/MONITORING AGENCY NAME(S) AND ADDRESS(ES)

AFRL/PRTC
Attn: Dr. Fred Schauer
1790 Loop Road
WPAFB OH 45433-7765
DSN: 785-6462
e-mail: frederick.schauer@wpafb.af.mil

10. SPONSOR/MONITOR'S ACRONYM(S)

11. SPONSOR/MONITOR'S REPORT NUMBER(S)

12. DISTRIBUTION/AVAILABILITY STATEMENT

APPROVED FOR PUBLIC RELEASE; DISTRIBUTION UNLIMITED.

13. SUPPLEMENTARY NOTES

14. ABSTRACT

Shock tubes utilize a difference in pressures between gases separated by a diaphragm to create a shock wave when the diaphragm ruptures. The AFIT 2-inch shock tube was reassembled and tested to ensure proper and safe operation. A high-speed data acquisition system was configured to take data at 2 MS/s. This research showed that the Mach number of the shock waves produced in this shock tube fall within 7% of theoretical values at speeds under Mach 3 and within 9% at higher speeds. The peak velocity of each shock wave was shown to occur at approximately 3 meters from the diaphragm. The second portion of the research focused on the testing of sensors used to evaluate the performance of the pulse detonation engine (PDE) for research and developmental purposes. Two alternatives were developed to standard sensors to withstand the heat of the engine: coat the sensors with an insulating, 0.6 mm thick silicone that protects it from the heat and use spark plugs as ion sensors to detect the ions in the combustion inside the PDE tubes. This researched proved that no degradation in response time, rise time, or sensitivity results from coating the pressure transducers with silicone. The research also found that the ion sensors are unable to consistently detect ions created by a Mach 8 shock wave through air.

15. SUBJECT TERMS

shock tube, pressure transducer, ion sensor probe, rtv silicone, pulse detonation engine, dissociation, ionization

16. SECURITY CLASSIFICATION OF:			17. LIMITATION OF ABSTRACT	18. NUMBER OF PAGES	19a. NAME OF RESPONSIBLE PERSON
a. REPORT	b. ABSTRACT	c. THIS PAGE			Dr. Paul I. King
U	**U**	**U**	**UU**	104	**19b. TELEPHONE NUMBER** *(Include area code)* (937)785-3636, ext 4628; e-mail: paul.king@afit.edu